Distributionally Robust Optimization for Chemotherapy Scheduling under Asymmetric and Multi-Modal Uncertainty

Qing Zhu* Xian Yu† Yu-Li Huang‡

Abstract

Problem definition: We consider a real-world chemotherapy scheduling template design problem, where we cluster patient types into groups and find a representative time-slot duration for each group to accommodate all patient types assigned to that group, aiming to minimize the total expected idle time and overtime. From Mayo Clinic's real data, most patients' treatment durations are asymmetric (e.g., shorter/longer durations tend to have a longer right/left tail). ***Methodology/results:*** Motivated by this observation, we consider a distributionally robust optimization (DRO) model under an asymmetric and multi-modal ambiguity set, where the distribution of the random treatment duration is modeled as a mixture of distributions from different patient types. The ambiguity set captures uncertainty in both the mode probabilities, modeled via a variation-distance-based set, and the distributions within each mode, characterized by moment information such as the empirical mean, variance, and semivariance. We reformulate the DRO model as a semi-infinite program, which cannot be solved by off-the-shelf solvers. To overcome this, we derive a closed-form expression for the worst-case expected cost and establish lower and upper bounds that are positively related to the variability of patient types assigned to each group, based on which we develop exact algorithms and highly efficient clustering-based heuristics. ***Managerial implications:*** The lower and upper bounds on the worst-case cost imply that the optimal cost tends to decrease if we group patient types with similar treatment times. Through numerical experiments based on both synthetic datasets and Mayo Clinic's real data, we illustrate the effectiveness and efficiency of the proposed exact algorithms and heuristics and showcase the benefits of incorporating asymmetric information into the DRO formulation.

Keywords: distributionally robust optimization, multimodal uncertainty, asymmetric uncertainty, moment-based ambiguity sets, chemotherapy scheduling

1 Introduction

Chemotherapy is one of the most resource-intensive services in ambulatory cancer units [20]. Each infusion in chemotherapy treatment requires nurses to perform a coordinated set of tasks—drug

*Department of Integrated Systems Engineering, The Ohio State University, Columbus, OH, USA, Email: zhu.2166@osu.edu;

†Corresponding author; Department of Integrated Systems Engineering, The Ohio State University, Columbus, OH, USA, Email: yu.3610@osu.edu;

‡Robert D. and Patricia E. Kern Center for the Science of Health Care Delivery, Mayo Clinic, Rochester, Minnesota, USA, Email: huang.yuli@mayo.edu;

verification, chair and line setup, patient education, infusion monitoring, and safe disconnection, resulting in highly uncertain treatment durations. The current scheduling procedure at the Mayo Clinic consists of two phases: (i) chemotherapy template design, where a fixed daily template (e.g., a 10-hour schedule on each chair) is optimized up front and will be implemented in the next several months (see Figure 1a), and (ii) chemotherapy patient scheduling, where patients are placed into the most appropriate available time slots as they call in to schedule their appointments sequentially. When no appropriate slot is available, the hospital operator combines two neighboring slots into a longer one or divides one longer slot into several shorter ones to fit the current patient, leading to the so-called "overrides" (see Figure 1b). In this paper, we mainly focus on Phase (i), where we optimize the duration of each contributing block in the daily template. Since these time-slot durations are decided before patients arrive and will be fixed through the next implementation horizon, they should be designed to accommodate variability in patient types and stochastic treatment lengths.

As demonstrated by Mayo Clinic's real data (See Figure 2 and Table 1), treatment durations exhibit wide variability. The hospital operator currently classifies all the patients into seven distinct types (e.g., 30-min type, 60-min type, etc.), based on their chemotherapy regimens, cancer subtypes, or characteristic patterns of comorbidities. Among these seven patient types, most treatment duration distributions are asymmetric. For example, Figure 2a shows that 30–minute infusions can extend substantially when adverse reactions occur, leading to a "right-skewed" or "positive-skewed" distribution. On the other hand, Figure 2g shows that 360–minute sessions sometimes finish earlier than planned, leading to a "left-skewed" or "negative-skewed" distribution. This asymmetric property of treatment duration distributions is further confirmed in Table 1, where we report the mean, standard deviation, and semivariance for each patient type. Note that a positive semivariance corresponds to a right-skewed distribution while a negative semivariance corresponds to a left-skewed distribution. This feature creates unique modeling challenges: shorter-than-expected sessions often leave nurses and medical resources idle, while longer-than-expected sessions can generate significant overtime. Both cases directly impact patient care quality and operational efficiency, which emphasizes the importance of explicitly capturing the skewness of treatment durations.

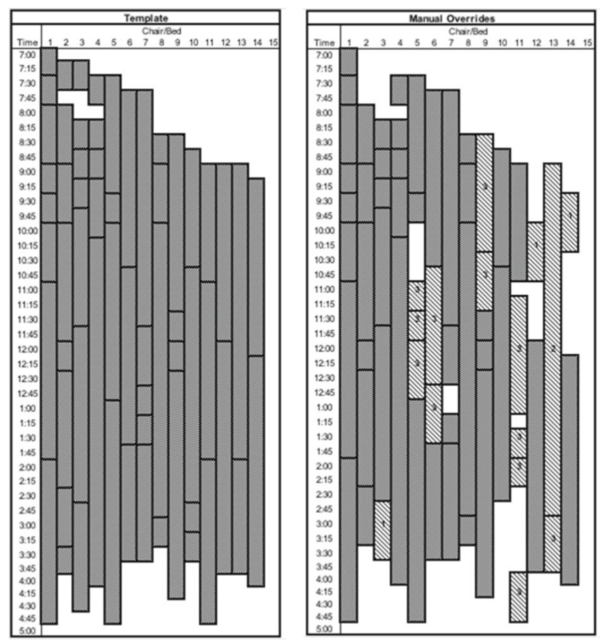

(a) Template (b) Override

Figure 1: Mayo Clinic example template

However, the current practice at the Mayo Clinic adopts a deterministic approach that ignores the randomness and skewness of the treatment durations. They use a specific time-slot duration to

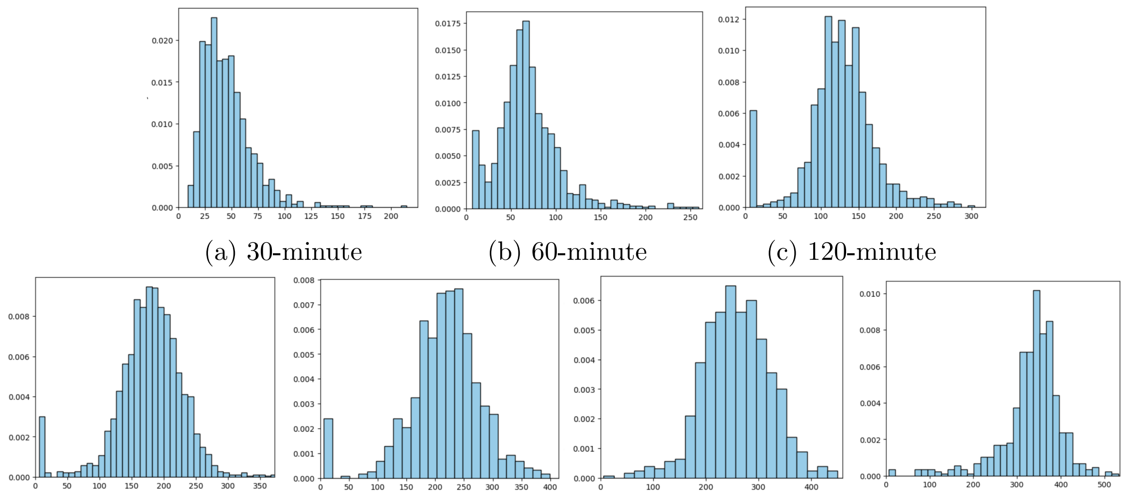

(a) 30-minute (b) 60-minute (c) 120-minute

(d) 180-minute (e) 240-minute (f) 300-minute (g) 360-minute

Figure 2: Histograms of treatment durations across seven patient types (Mayo Clinic's real data).

Table 1: Statistics of treatment durations across seven patient types (Mayo Clinic's real data)

Patient Type	**Count**	**Proportion**	**Mean**	**Std**	**Semivariance**
30-min	923	13.83%	48.70	31.15	0.59
60-min	1013	15.18%	73.24	39.65	0.47
120-min	913	13.69%	133.88	42.98	0.33
180-min	1851	27.74%	182.87	47.20	0.07
240-min	745	11.17%	223.34	57.07	0.07
300-min	641	9.61%	258.78	65.27	−0.005
360-min	586	8.78%	336.29	66.66	−0.25

accommodate one patient type (e.g., 30-min time slots designed solely for 30-min patient type). The issues of such a deterministic approach are two-fold. First, once a schedule template is fixed (see Figure 1a), we have a certain number of time slots for each patient type (e.g., 23 30-min time slots, 8 60-min time slots, 10 120-min time slots, etc.). Given the stochastic nature of the patient counts in each type, if the realized count of each patient type exceeds the allocated number of time slots, this may result in excessively large overrides. Second, the deterministic approach fails to capture the asymmetry of the random treatment durations, as reflected in Figure 2, which may result in substantial idle time and overtime in practice. Overall, ignoring the randomness and skewness of the treatment durations when designing templates could potentially lead to significant inefficiencies in resource utilization and compromised patient care quality.

In this paper, we adopt a stochastic approach that treats the treatment duration for each patient type as a random variable and explicitly captures its asymmetric information by using second-order statistics (e.g., semivariance). We propose a general framework to consolidate all patient types into a smaller number of groups, designing a representative time-slot duration for each group, such that each duration can accommodate all patient types assigned to that group.

We formulate this chemotherapy patient grouping and time-slot duration design problem as a Multimodal Asymmetric Distributionally Robust Optimization (MMA-DRO) model that accounts for (i) multimodal uncertainty, by representing each patient group's treatment time distribution as a mixture of the distributions of the patient types assigned to that group, and (ii) asymmetric information, by incorporating semivariance information into the ambiguity set for each group. Specifically, the model determines patient-type-to-grouping assignments and the time-slot duration within each group to minimize the group activation cost and the worst-case expected cost of idle time and overtime. Given the assignment decisions, each group finds the optimal time-slot duration against the worst-case scenario within a multi-modal and asymmetric ambiguity set. This data-driven formulation allows us to create more flexible scheduling templates by consolidating multiple patient types and assigning each duration to accommodate the skewness of treatment time distributions from several patient types, potentially reducing idle time, overtime, and overrides in real-world practice.

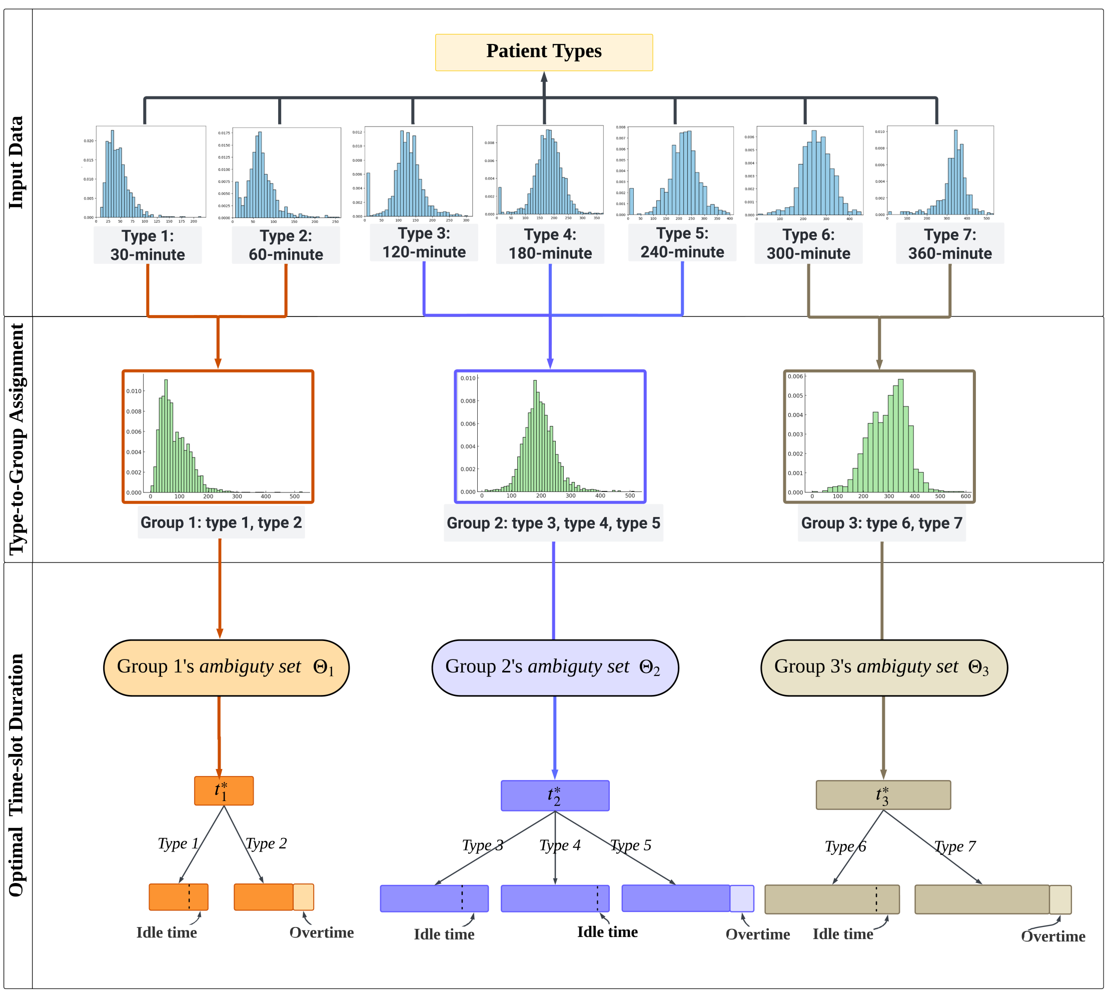

Figure 3: A flowchart of the MMA-DRO model, where Θ_1, Θ_2, Θ_3 denote the multimodal asymmetric ambiguity sets of the uncertain chemotherapy durations and t_1^*, t_2^*, t_3^* denote the optimal time-slot durations for groups 1, 2, 3, respectively.

The resulting MMA-DRO model is highly non-convex, as our first-stage assignment decisions can affect the ambiguity sets in a complicated form, leading to decision-dependent ambiguity sets. Using strong duality, we recast the MMA-DRO model as a monolithic minimization problem; however, since we consider a continuous support set for the uncertainty, this results in a semi-infinite program. To overcome the intractability of having infinitely many constraints, we first derive a closed-form expression for the worst-case cost of idle time and overtime given any assignment decision, using which we design exact algorithms to solve this semi-infinite program by enumerating all possible assignments. We also establish both lower and upper bounds on each group's optimal cost, which are positively related to the variability of patient types assigned to that group. This managerial insight further motivates us to leverage clustering approaches (e.g., K-Means and K-Medoids algorithms) to find a near-optimal assignment decision first and then embed it into the closed-form expression to optimize the time-slot durations in a quick fashion.

The remainder of the paper is organized as follows. Section 1.1 reviews the relevant DRO and healthcare scheduling literature, highlighting the existing gaps in modeling multimodality and asymmetry under the DRO framework. Section 2 presents our problem formulation and derives a monolithic semi-infinite program using strong duality. Section 3 introduces exact algorithms to solve the resulting semi-infinite program by using a closed-form expression of the worst-case expected cost of idle time and over time and establishes the lower and upper bounds on each group's optimal cost. Motivated by this insight, Section 4 develops highly efficient heuristics to obtain near-optimal solutions by leveraging clustering approaches (e.g., K-Means and K-Medoids algorithms). In Section 5, we report experimental results based on synthetic datasets to conduct sensitivity analyses and out-of-sample tests, and in Section 6, we present a case study based on Mayo Clinic's real chemotherapy data. Finally, Section 7 discusses managerial insights and directions for future research.

1.1 Related Work

Chemotherapy scheduling under uncertainty. We first review the most relevant literature that applies optimization under uncertainty techniques to solve the chemotherapy scheduling problem. Stochastic programming (SP) emerges as one of the most widely employed frameworks in optimization under uncertainty, which aims to optimize the system performance on average or based on a risk measure. For instance, [8, 13, 1, 25, 16] proposed two-stage stochastic mixed-integer programs to optimize patient appointment schedules under uncertain treatment durations. Among these papers, decisions include the sequence of patients on a daily schedule, their appointment starting times, patient-to-nurse/chair assignments, and clinic resource schedules. The objective is often set to minimize a trade-off between the expected cost of patient waiting time, chair idle time, and nurse overtime. To solve these problems, they developed both exact and heuristic methods, based on progressive hedging [13], scenario bundling-based decomposition [25, 16], etc. Robust optimization (RO), on the other hand, aims to find the optimal decisions against the worst-case scenario within a pre-defined uncertainty set, without access to the probability distributions. Numerous studies have shown its suitability to handle uncertain treatment durations and operational disruptions in chemotherapy scheduling [22, 5, 3]. [3] and [5] considered box uncertainty sets to model random appointment durations and no-shows, and service quality, respectively, where [22] proposed a Robust Slack Allocation model by inserting a slack variable to each uncertain constraint. To solve the RO models, [22] developed a heuristic based on adaptive large neighborhood search, [5] proposed a multi-objective particle swarm optimization heuristic, and [3] explored the structural property and reformulated the RO model as a compact mixed-integer linear program. More recently, DRO has become a powerful framework that bridges SP and RO by optimizing decisions against the worst-case expected performance over an ambiguity set of probability distributions. Recent advances have extended DRO to address chemotherapy scheduling challenges. [18] developed a DRO framework for radiation therapy treatment planning that accounts for inter-fraction geometric uncertainty of the clinical target volume. [2] adopted a DRO model to solve a scheduling problem that requires coordination between clinical and surgical appointments, where they considered two sources of uncertainty: (i) the patient may or may not need surgery after the clinical appointment and (ii) the surgery duration for each patient and procedure is unknown. [26] proposed an integrated multi-stage stochastic and DRO framework to jointly schedule clinical and surgical appointments under uncertainties in appointment demand, surgery necessity, and surgery durations to minimize overtime. [33] proposed a DRO framework to determine optimal appointment sequences and minimize the worst-case sum of patient waiting, provider idling, and overtime. Different than the aforementioned papers, which optimize patient appointment start times at any minute, our paper considers a fixed template with pre-determined time slots, which can fit the patients into the most appropriate time slots as they call in to schedule. The use of pre-determined time slots facilitates both the construction of a scheduling template and the real-time assignment of patients to time slots. To the best of our knowledge, only [19] studied a chemotherapy scheduling template design problem; however, they considered a deterministic setting and the time-slot durations are fixed at 30 minutes, 60 minutes, 120 minutes, etc. Instead, the main focus of this paper is to optimize the durations of the contributing blocks in such a template, while considering the asymmetric property of the treatment time distributions.

Modeling asymmetric uncertainty. To model asymmetric uncertainty, [11] introduced a robust optimization approach for constructing asymmetric uncertainty sets using forward and backward deviation measures of random variables. [29] then extended it to incorporate asymmetric distributional information in a modified Value-at-Risk (VaR) measure, named Asymmetry-Robust VaR (ARVaR), and proposed a computationally tractable approximation method for minimizing the ARVaR of a portfolio based on robust optimization techniques. In DRO, traditional approaches to constructing ambiguity sets generally fall into two categories: (i) moment-based ambiguity sets [12, 27, 35, 38, 37], which are defined using information about the moments of the distribution (e.g., mean, variance, or higher-order moments), and (ii) distance-based ambiguity sets [14, 6, 15, 24, 23, 4], which are formed by measuring the distance between the empirical distribution and alternative distributions under a chosen metric (e.g., Wasserstein distance or ϕ-divergence). These DRO models, however, often fail to account for the inherent skewness or asymmetric tail behavior of the uncertainty, which limits their effectiveness in modeling the treatment time distributions. Several recent works have addressed this gap by directly integrating asymmetry information into the ambiguity sets. [30] constructed the ambiguity set with mean, variance, and semivariance information to account for the asymmetric demand distribution when solving a newsvendor problem. [10] introduced a general moment-dispersion ambiguity set by incorporating a dispersion characteristic function, which can capture the uncertainty's complex attributes, such as sub-Gaussian and asymmetric dispersion. [9] developed a distributionally robust pricing model to optimize the worst-case profit, where they used semivariance to capture the asymmetric information of the consumers' valuation distribution.

Modeling multimodal uncertainty. We now turn our attention to recent DRO studies that have emphasized modeling multimodal uncertainty, which is characterized by distributions composed of distinct probability modes and their associated distributional information. [17] addressed a risk-averse, multi-dimensional newsvendor problem through a DRO formulation that captures multimodal demand distributions represented by spatially separated probability clusters. Building on this direction, [36] introduced a general two-stage DRO model under multimodal decision-dependent ambiguity sets, where the first-stage decisions could affect both the mode probabilities and the corresponding distributions in each mode. To model bimodal demand distributions in facility location problems, [34] constructed a scenario-based DRO model that captures the ambiguity of the bimodal demand to optimize the number and location of the facilities. Moreover, [33] considered an outpatient colonoscopy scheduling problem and modeled the colonoscopy durations as bimodal distributions in a DRO framework to determine optimal appointment sequences, minimizing the worst-case expected cost of patient waiting, provider idling, and overtime. In a complementary line of research within machine learning, [31] proposed a group DRO approach to minimize the worst-case expected loss of predictive models over mixtures of predefined distributions, which effectively captured potential multimodalities present in the test data distribution.

To the best of our knowledge, no existing studies have addressed the chemotherapy scheduling template design problem while considering multimodal and asymmetric uncertainty. This paper aims to bridge this gap by introducing an MMA-DRO framework that groups multiple patient types and optimizes the time-slot duration within each group to accommodate the skewness of treatment time distributions assigned to this group.

1.2 Contributions

We summarize the main contributions of this paper as follows:

1. We formulate the chemotherapy patient grouping and time-slot duration design problem as a distributionally robust optimization (DRO) model, under asymmetric and multi-modal ambiguity sets. Specifically, we optimize the assignment of different patient types to groups and decide the duration of time slots for each group to accommodate various patient types assigned to this group.

2. Under a continuous support set of the uncertainty, we reformulate the DRO model as a

monolithic semi-infinite program, which cannot be solved via standard optimization solvers. To overcome this, we derive a closed-form expression for the inner maximization problem, based on which we develop two exact algorithms to solve the DRO model by enumerating all possible patient type-to-group assignment decisions.

3. To obtain managerial insight into optimal grouping assignments, we provide lower and upper bounds for each group's optimal cost, which both depend on the difference between the maximum and minimum average treatment time among all the patient types assigned to this group. This implies that the optimal cost tends to decrease if we group patient types with similar treatment times.

4. Motivated by the above insights, we propose to use K-means clustering algorithms to find a near-optimal assignment based on the similarity of different statistics across all patient types. Once the assignment is given, we leverage the closed-form expression of the inner maximization problem again to find the optimal appointment duration for each group.

5. Finally, we validate our approach through numerical experiments on both real-world Mayo Clinic data and synthetic datasets.. The results demonstrate that explicitly modeling multi-modality and asymmetry within the ambiguity set significantly improves the robustness and efficiency of chemotherapy treatment–template design.

2 Problem Formulations

Let $\tilde{\xi} \in \Xi$ represent the random chemotherapy treatment duration that follows an underlying (unknown) distribution $\mathcal{P}$ with a compact support set Ξ (in this paper, we consider a bounded and continuous support set Ξ). Let $\mathcal{L} = \{1, 2, \ldots, L\}$ denote a set of patient types depending on specific chemotherapy regimens or cancer types (e.g., 30-min type, 60-min type, etc.), and $\mathcal{G} = \{1, 2, \ldots, G\}$ denote a set of potential patient groups. Note that G can be set to L to represent the maximum number of groups one can create, or it can be set to a lower number depending on the operational constraints and the decision maker's preference. Define x_{lg} as a binary decision variable indicating if the patient type $l \in \mathcal{L}$ is assigned to the group $g \in \mathcal{G}$, and y_g as a binary decision variable indicating whether the group $g \in \mathcal{G}$ is activated or not. Let $t_g \in \mathcal{T} := [0, T]$ be the time-slot duration to be determined for each group $g \in \mathcal{G}$, which will serve for all the patient types assigned to this group. The upper bound T for the time-slot duration can be set to the maximum treatment time or set according to some operational constraints (e.g., 5 hours due to limited nurse resources). Throughout the paper, we use a^+ to denote $\max\{0, a\}$ and use bold symbols to denote vectors.

Let q, b, and c_g represent the unit cost of overtime, idle time, and activating group $g \in \mathcal{G}$, respectively. Specifically, q is the unit penalty on the overtime when actual chemotherapy durations exceed their scheduled time-slot durations (i.e., $\tilde{\xi} \geq t_g$), and b is the unit penalty on the idle time when treatments conclude earlier than scheduled (i.e., $t_g \geq \tilde{\xi}$). The unit group-activating cost c_g can be set the same across all groups g, so that the term $\sum_g c_g y_g$ penalizes the total number of groups. When c_g is set to be a larger value, it encourages a smaller number of activated groups so that each group will accommodate more patient types. This creates a natural trade-off between the number of activated groups and the overall system performance.

Our goal is to simultaneously determine the optimal assignment of patient types to groups and the corresponding time-slot duration within each group in order to minimize the overall cost incurred by overtime, idle time, and group activation. To formulate this problem, we adopt the following MMA-DRO framework:

$$\min_{x_{lg},y_g,t_g} \quad \left\{ \sum_{g\in\mathcal{G}} c_g y_g + \frac{1}{\sum_{g\in\mathcal{G}} y_g} \sum_{g\in\mathcal{G}} \max_{P\in\Theta_g(\boldsymbol{x},\boldsymbol{y})} \mathbb{E}_{\tilde{\xi}\sim P}\left[q(\tilde{\xi}-t_g)^+ + b(t_g-\tilde{\xi})^+ \right] \right\} \tag{1a}$$

$$\text{s.t.} \quad \sum_{g\in\mathcal{G}} x_{lg} = 1,\ \forall l\in\mathcal{L} \tag{1b}$$

$$x_{lg} \le y_g,\ \forall l\in\mathcal{L},\ g\in\mathcal{G} \tag{1c}$$

$$\sum_{l=1}^{L} x_{lg} \ge y_g,\ \forall g\in\mathcal{G} \tag{1d}$$

$$0 \le t_g \le T,\ \forall g\in\mathcal{G}, \tag{1e}$$

where we aim to minimize the fixed cost of activating groups together with the worst-case expected cost of idle time and overtime, averaged over the activated groups in Eq. (1a). Constraints (1b) ensure that each patient type is assigned to exactly one group. Constraints (1c) ensure that patient types can only be assigned to groups that are activated. Constraints (1d) enforce that every activated group must have at least one patient type assigned to it, which eliminates empty groups. Constraints (1e) put a lower and upper bound on the time-slot duration t_g for each $g\in\mathcal{G}$.

Given the group activation and assignment decisions $(\boldsymbol{x},\boldsymbol{y})$, within each group g, we consider a multi-modal ambiguity set $\Theta_g(\boldsymbol{x},\boldsymbol{y})$ to capture the uncertainty in treatment-time distributions, where each patient type in the group is treated as a possible mode l, weighted by its proportion within the group, referred to as the mode probability p_l. Following [36], we adopt a two-layer ambiguity set to describe $\Theta_g(\boldsymbol{x},\boldsymbol{y})$, where the first layer captures the uncertainty in mode probabilities and the second layer represents the uncertainty around the distribution in each mode. Specifically, for each $g\in\mathcal{G}$, any candidate distribution $P\in\Theta_g(\boldsymbol{x},\boldsymbol{y})$ can be represented as a mixture of distributions from each mode weighted by the mode probability as follows:

$$\Theta_g(\boldsymbol{x},\boldsymbol{y}) = \left\{ P = \sum_{l=1}^{L} p_l\, f_l :\ \underbrace{\boldsymbol{p}\in\Delta_g(\hat{\boldsymbol{p}},\boldsymbol{x},\boldsymbol{y})}_{\text{mode probability vector}},\quad \underbrace{f_l\in U_l,\ \forall l\in\mathcal{L}}_{\text{distribution in each mode}} \right\}. \tag{2}$$

Here, the probability vector $\boldsymbol{p}=(p_1,\ldots,p_L)^\mathsf{T}$ corresponds to the proportion of each patient type within the group. We use the proportion of each patient type l in the Mayo Clinic's dataset to construct a nominal probability $\hat{p}_l$ for each $l\in\mathcal{L}$ (i.e., the "Proportion" column in Table 1). Then, according to the group activation and assignment decisions $(\boldsymbol{x},\boldsymbol{y})$, we adopt a decision-dependent variation distance-based ambiguity set $\Delta_g(\hat{\boldsymbol{p}}, \boldsymbol{x}, \boldsymbol{y})$ as follows:

$$\Delta_g(\hat{\boldsymbol{p}}, \boldsymbol{x}, \boldsymbol{y}) = \left\{ \boldsymbol{p} \in \mathbb{R}_+^L : p_l \leq x_{lg},\ \sum_{l=1}^{L} \left| p_l (\sum_{l=1}^{L} x_{lg}\hat{p}_l) - x_{lg}\hat{p}_l \right| \leq \rho \sum_{l=1}^{L} x_{lg}\hat{p}_l,\ \sum_{l=1}^{L} p_l = y_g \right\}. \quad (3)$$

For a given group $g \in \mathcal{G}$, this formulation restricts mode probabilities $\boldsymbol{p}$ to deviate from the nominal ones within a radius ρ. In particular, if group g is not activated ($y_g = 0$), then no patient type is assigned to this group ($x_{lg} = 0,\ \forall l \in \mathcal{L}$), which enforces all mode probabilities to be 0, i.e., $p_l = 0,\ \forall l \in \mathcal{L}$. As a result, this group will not contribute any idle time or overtime. If group g is activated ($y_g = 1$), the nominal probability for type l within group g is given by the conditional distribution $\frac{x_{lg}\hat{p}_l}{\sum_{l=1}^{L} x_{lg}\hat{p}_l}$, which rescales the proportions $\hat{p}_l$ so that they sum to one across all patient types assigned to group g. Dividing both sides of the second condition in (3) by $\sum_{l=1}^{L} x_{lg}\hat{p}_l$, we require the total variation distance between the mode probability p_l and the nominal one $\frac{x_{lg}\hat{p}_l}{\sum_{l=1}^{L} x_{lg}\hat{p}_l}$ for all $l = 1, \ldots, L$ to be within ρ. Moreover, when patient type l is not assigned to the group g ($x_{lg} = 0$), the corresponding probability p_l must be zero.

Given a mode l, the second layer characterizes the uncertainty within each mode l by describing the random duration through the unknown density f_l that belongs to a moment-based ambiguity set U_l. To capture the asymmetric information of the duration distribution within each mode, we follow [30] by including a second-order statistic (i.e., semivariance). For any random variable $\tilde{\xi}$, the normalized semivariance is defined as $s = \frac{\mathbb{E}\left[\left((\tilde{\xi}-m)^+\right)^2\right] - \mathbb{E}\left[\left((m-\tilde{\xi})^+\right)^2\right]}{\sigma^2}$, where m denotes the mean of $\tilde{\xi}$ and σ denotes the standard deviation of $\tilde{\xi}$. The normalized semivariance s captures asymmetry by measuring the imbalance between the variability above and below the mean m. A positive s indicates a right-skewed distribution, while a negative s corresponds to a left-skewed distribution. Consequently, we define the asymmetric moment-based ambiguity set U_l as

$$U_l := \left\{ f_l \in \mathcal{P}(\Xi) : \mathbb{E}_{f_l}\left[\tilde{\xi}\right] = m_l,\ \mathbb{E}_{f_l}\left[(\tilde{\xi} - m_l)^2\right] = \sigma_l^2,\ \mathbb{E}_{f_l}\left[(\tilde{\xi} - m_l)^{+2}\right] - \mathbb{E}_{f_l}\left[(m_l - \tilde{\xi})^{+2}\right] = s_l\sigma_l^2 \right\}, \quad (4)$$

where the parameters $m_l,\ \sigma_l$ and s_l represent the mean, variance, and normalized semivariance of $\tilde{\xi}$ in mode l, respectively, and $\mathcal{P}(\Xi)$ denotes all the probability distributions supported on Ξ. This layer of ambiguity captures the essential second-order information and asymmetric tail behavior of the distribution of chemotherapy duration.

Under the ambiguity set (2), we further reformulate our Problem (1) as

$$\min_{x_{lg}, y_g, t_g} \quad \left\{ \sum_{g \in \mathcal{G}} c_g y_g + \frac{1}{\sum_{g \in \mathcal{G}} y_g} \sum_{g \in \mathcal{G}} \max_{\boldsymbol{p} \in \Delta_g(\hat{\boldsymbol{p}}, \boldsymbol{x}, \boldsymbol{y})} \sum_{l=1}^{L} p_l \max_{f_l \in U_l} \mathbb{E}_{\tilde{\xi} \sim f_l} \left[q(\tilde{\xi} - t_g)^+ + b(t_g - \tilde{\xi})^+ \right] \right\} \quad (5)$$

$$\text{s.t.} \quad \text{Constraints (1b), (1c), (1d), (1e).}$$

To better represent the problem formulation, we first denote the innermost maximization problem (i.e., worst-case cost of idle time and overtime) in Problem (5) for a given group g and mode l as

$$\Pi_l(t_g) := \max_{f_l \in U_l} \mathbb{E}_{\tilde{\xi} \sim f_l} \left[q(\tilde{\xi} - t_g)^+ + b(t_g - \tilde{\xi})^+ \right], \tag{6}$$

and make the following assumption to derive a dual representation of $\Pi_l(t_g)$.

Assumption 1. For each type $l \in \mathcal{L}$, the treatment duration has mean $m_l > 0$, standard deviation $\sigma_l > 0$ and normalized semivariance s_l satisfying $s_l \in \left[\frac{\sigma_l^2 - m_l^2}{\sigma_l^2 + m_l^2}, 1\right)$.

According to Proposition 2.1 in [30], Assumption 1 provides a necessary and sufficient condition on the mean, standard deviation, and normalized semivariance of a nonnegative random variable, which ensures that the ambiguity set U_l is non-empty.

In the following theorem, we present a dual representation of $\Pi_l(t_g)$. Throughout the paper, all the proofs are presented in Appendix A.

Theorem 1 (Dual representation of $\Pi_l(t_g)$)**.** Under Assumption 1, $\Pi_l(t_g)$ admits the following dual formulation

$$\begin{aligned}
\Pi_l(t_g) = \min_{\gamma_{lg}, \nu_{lg}, \kappa_{lg}, \zeta_{lg}} \quad & \gamma_{lg} + \nu_{lg} m_l + \kappa_{lg} \sigma_l^2 + \zeta_{lg} s_l \sigma_l^2 \\
\text{s.t.} \quad & \gamma_{lg} + \nu_{lg} \tilde{\xi} + \kappa_{lg} (\tilde{\xi} - m_l)^2 + \zeta_{lg} \Big((\tilde{\xi} - m_l)^{+2} - (m_l - \tilde{\xi})^{+2} \Big) \\
& \geq q(\tilde{\xi} - t_g)^+ + b(t_g - \tilde{\xi})^+, \quad \forall \tilde{\xi} \in \Xi, \\
& \gamma_{lg}, \nu_{lg}, \kappa_{lg}, \zeta_{lg} \in \mathbb{R}.
\end{aligned} \tag{7}$$

Next, we investigate the overall maximization problem by including the mode probability ambiguity set $\Delta_g(\hat{\boldsymbol{p}}, \boldsymbol{x}, \boldsymbol{y})$. For each group $g \in \mathcal{G}$, we denote

$$\Omega_g(t_g) := \max_{\boldsymbol{p} \in \Delta_g(\hat{\boldsymbol{p}}, \boldsymbol{x}, \boldsymbol{y})} \sum_{l=1}^{L} p_l \Pi_l(t_g),$$

and derive its dual representation in the next theorem.

Theorem 2 (Dual representation of $\Omega_g(t_g)$)**.** Under Assumption 1, $\Omega_g(t_g)$ admits the following dual formulation

$$\Omega_g(t_g) = \min_{\mu_g, \lambda_{lg}, \tau_g, \alpha_l, \beta_l} \quad \mu_g y_g + \sum_{l=1}^{L} \lambda_{lg} x_{lg} + \sum_{l=1}^{L} (\alpha_{lg} - \beta_{lg}) \hat{p}_l x_{lg} + \rho \tau_g \sum_{l=1}^{L} x_{lg} \hat{p}_l \tag{8a}$$

$$\text{s.t.} \quad \mu_g + \lambda_{lg} + (\alpha_{lg} - \beta_{lg}) (\sum_{l=1}^{L} x_{lg} \hat{p}_l) \geq \Pi_l(t_g), \ \forall l \in \mathcal{L} \tag{8b}$$

$$-\alpha_{lg} - \beta_{lg} + \tau_g \geq 0, \ \forall l \in \mathcal{L} \tag{8c}$$

$$\mu_g \in \mathbb{R}, \ \lambda_{lg}, \ \alpha_{lg}, \ \beta_{lg}, \ \tau_g \geq 0. \tag{8d}$$

Combining Theorems 1 and 2, we derive a monolithic minimization problem of our MMA-DRO model (1) as follows

$$\min \quad \left\{ \sum_{g\in\mathcal{G}} c_g y_g + \frac{1}{\sum_{g\in\mathcal{G}} y_g} \sum_{g\in\mathcal{G}} \Big(\mu_g y_g + \sum_{l=1}^{L} \lambda_{lg} x_{lg} + \sum_{l=1}^{L} (\alpha_{lg} - \beta_{lg}) \hat{p}_l x_{lg} + \tau_g (\rho \sum_{l=1}^{L} x_{lg} \hat{p}_l) \Big) \right\}$$

$$\text{s.t.} \quad \mu_g + \lambda_{lg} + (\alpha_{lg} - \beta_{lg})(\sum_{l=1}^{L} x_{lg}\hat{p}_l) \geq \gamma_{lg} + \nu_{lg} m_l + \kappa_{lg}\sigma_l^2 + \zeta_{lg} s_l \sigma_l^2, \ \forall l \in \mathcal{L}, \ g \in \mathcal{G} \tag{9a}$$

$$\gamma_{lg} + \nu_{lg}\tilde{\xi} + \kappa_{lg}(\tilde{\xi} - m_l)^2 + \zeta_{lg}\left((\tilde{\xi} - m_l)^{+2} - (m_l - \tilde{\xi})^{+2} \right) \geq q(\tilde{\xi} - t_g)^+ + b(t_g - \tilde{\xi})^+, \ \forall l \in \mathcal{L}, \ \forall g \in \mathcal{G}, \ \forall \tilde{\xi} \in \Xi \tag{9b}$$

$$-\alpha_{lg} - \beta_{lg} + \tau_g \geq 0, \ \forall l \in \mathcal{L}, \ g \in \mathcal{G} \tag{9c}$$

$$\text{Constraints (1b), (1c), (1d), (1e)}$$

$$\gamma_{lg}, \ \nu_{lg}, \ \kappa_{lg}, \ \zeta_{lg}, \ \mu_g \in \mathbb{R}, \ \lambda_{lg}, \ \alpha_{lg}, \ \beta_{lg}, \ \tau_g, \ t_g \geq 0 \tag{9d}$$

$$x_{lg}, \ y_g \in \{0, 1\}, \ \forall l \in \mathcal{L}, \ g \in \mathcal{G} \tag{9e}$$

This formulation, however, results in an intractable semi-infinite optimization problem due to the continuous support set Ξ in Constraints (9b), thereby preventing the direct use of standard optimization solvers. To overcome this intractability, we first derive a closed-form expression for $\Pi_l(t_g)$, based on which we develop two exact algorithms for solving this semi-infinite program (9) in Section 3. Although these exact algorithms guarantee to find optimal solutions, they become computationally expensive when the problem size increases. To further improve the computational time, in Section 4, we develop several heuristics based on clustering algorithms (e.g., K-Means and K-Medoids), which can find near-optimal solutions in a quick fashion. We also consider a generalized ambiguity set U_l that allows the mean, variance, and semivariance to deviate from the empirical ones within a given radius and derive its corresponding dual form under a discrete support set in Appendix D. We will compare it with other benchmarks in Section 5.

3 Exact Algorithms for Solving MMA-DRO Model (9)

In the semi-infinite program (9), the challenging part lies in Constraints (9a)–(9b) (or, equivalently, Constraints (8b)), which involve the worst-case expected cost $\Pi_l(t_g)$ for mode l in group g. In this section, we first derive a closed-form expression for $\Pi_l(t_g)$, which takes the form of a piecewise convex function in t_g. Then given a specific assignment decision $(\boldsymbol{x}, \boldsymbol{y})$, we leverage this closed-form expression to develop an exact algorithm to solve the semi-infinite program (9) by exploiting its first-order conditions when $\rho = 0$ (i.e., the variation distance set (3) reduces to a singleton) in Section 3.1. When $\rho \neq 0$, we replace the right-hand side of (9a) and Constraint (9b) using the closed-form expression of $\Pi_l(t_g)$ and develop an exact algorithm to solve (9) in Section 3.2.

Specifically, given an assignment decision $(\boldsymbol{x}, \boldsymbol{y})$, Problem (1) can be decomposed by group g

and each group g needs to solve the following min-max problem

$$\min_{t_g \in \mathcal{T}} \max_{\boldsymbol{p} \in \Delta_g(\hat{\boldsymbol{p}}, \boldsymbol{x}, \boldsymbol{y})} \sum_{l=1}^{L} p_l \Pi_l(t_g). \tag{10}$$

Next, we derive a closed-form expression for $\Pi_l(t_g)$ in Theorem 3.

Theorem 3. Under Assumption 1, $\Pi_l(t_g)$ admits the following closed-form expression for each mode l and group g:

$$\begin{aligned}
&\Pi_l(t_g) = f_{l1}(t_g) := \left(\frac{(b+q)(1-s_l)\sigma_l^2}{2m_l^2} - q \right) t_g + q m_l, \text{ if } t_g \in \mathcal{T}_{l1} := \left[0, \frac{m_l}{2}\right] \\
&\Pi_l(t_g) = f_{l2}(t_g) := \frac{(b+q)(1-s_l)\sigma_l^2}{8(m_l - t_g)} - q t_g + q m_l, \text{ if } t_g \in \mathcal{T}_{l2} := \left[\frac{m_l}{2}, m_l - \frac{\sigma_l}{2}\sqrt{\frac{1-s_l}{1+s_l}}\right] \\
&\Pi_l(t_g) = f_{l3}(t_g) := \frac{(b+q)\sigma_l}{2}\sqrt{1-s_l^2} + (m_l - t_g)\frac{(q-b)-(q+b)s_l}{2}, \\
&\qquad\qquad \text{if } t_g \in \mathcal{T}_{l3} := \left[m_l - \frac{\sigma_l}{2}\sqrt{\frac{1-s_l}{1+s_l}}, m_l + \frac{\sigma_l}{2}\sqrt{\frac{1+s_l}{1-s_l}}\right] \\
&\Pi_l(t_g) = f_{l4}(t_g) := \frac{(b+q)(1+s_l)\sigma_l^2}{8(t_g - m_l)} + b t_g - b m_l, \text{ if } t_g \in \mathcal{T}_{l4} := \left[m_l + \frac{\sigma_l}{2}\sqrt{\frac{1+s_l}{1-s_l}}, m_l + \frac{m_l(1+s_l)}{2(1-s_l)}\right] \\
&\Pi_l(t_g) = f_{l5}(t_g) := b t_g + q m_l - \frac{b+q}{2}\left[m_l + \beta_l t_g - (t_g - m_l)\sqrt{\beta_l\left(\beta_l + \frac{m_l w_{1l} - 2 w_{2l}(t_g - m_l)}{m_l (t_g - m_l)^2}\right)}\right], \\
&\qquad\qquad \text{if } t_g \in \mathcal{T}_{l5} := \left[m_l + \frac{m_l(1+s_l)}{2(1-s_l)}, T\right].
\end{aligned} \tag{11}$$

where $w_{1l} = \frac{(1+s_l)\sigma_l^2}{2}, \; w_{2l} = \frac{(1-s_l)\sigma_l^2}{2}, \; \beta_l = 1 - \frac{(1-s_l)\sigma_l^2}{2m_l^2}$.

The proof of Theorem 3 is shown in Appendix A.3, which consists of constructing a dual feasible solution and a primal feasible distribution with the same objective values. By strong duality, this establishes optimality. The construction reduces to analyzing the relationship between the piecewise function $\Pi_l(t_g)$ and the quadratic function of the dual formulation of the ambiguity set U_l.

Note that in Theorem 3, for each mode l, we partition the feasible set $\mathcal{T}$ into five pieces $\mathcal{T}_{li}, \; i = 1, \ldots, 5$ and derive a closed-form expression for $\Pi_l(t_g)$ on each piece, i.e., $f_{li}(t_g), \; i = 1, \ldots, 5$. From the primal formulation in (6), we observe that $\Pi_l(t_g)$ is convex in t_g because maximum and expectation operators preserve convexity. Therefore, these five pieces $f_{li}(t_g), \; i = 1, \ldots, 5$ are linear or convex functions in t_g.

3.1 $\rho = 0$

When we are confident in the nominal mode probability estimated from the real-world dataset, we can set $\rho = 0$. In this case, the ambiguity set (3) collapses to a singleton, i.e., $p_l = \frac{x_{lg}\hat{p}_l}{\sum_{l=1}^{L} x_{lg}\hat{p}_l}, \; \forall l \in \mathcal{L}$ and Problem (10) becomes $\min_{t_g \in \mathcal{T}} \Pi(t_g) := \sum_{l=1}^{L} p_l \Pi_l(t_g)$.

Since each $\Pi_l(t_g)$ is a piece-wise convex function with intervals $\mathcal{T}_{li}$ for $i = 1, \ldots, 5$, taking a convex combination of $\Pi_l(t_g)$ for all $l = 1, \ldots, L$ leads to a convex function $\Pi(t_g)$. All such intervals $\bigcup_{\substack{l:\, x_{lg}=1 \\ i=1,\ldots,5}} \{\mathcal{T}_{li}\}$ will partition the feasible set $\mathcal{T}$ into disjoint intervals $\{\mathcal{T}_j\}_{j=1}^{J}$, where $\mathcal{J}$ denotes the total number of pieces in $\Pi(t_g)$. For each interval $\mathcal{T}_j$, we construct an explicit representation of $\Pi(t_g)$, using the closed-form expression in $\Pi_l(t_g)$. Consequently, the optimal solution t_g^* can be characterized by the subgradient optimality condition, i.e. $0 \in \partial_{t_g}\Pi(t_g^*) + \mathcal{N}_{\mathcal{T}}(t_g^*)$, where $\partial_x f(x)$ denotes the subgradient of $f(x)$ at x and $\mathcal{N}_{\mathcal{T}}(t_g^*)$ denotes the normal cone of $\mathcal{T}$.

Theorem 4. [Convexity and global optimality condition.] $\Pi(t_g)$ is convex in t_g, and t_g^* is optimal if and only if $0 \in \partial_{t_g}\Pi(t_g^*) + \mathcal{N}_{\mathcal{T}}(t_g^*)$. Specifically, the optimal solution t_g^* is either obtained at a stationary point of one of the convex function pieces or at one of the endpoints of all intervals $\{\mathcal{T}_j\}_{j=1}^{J}$.

According to Theorem 4, we transition from solving the intractable semi-infinite problem (9) to a simple root-finding problem, which is more computationally efficient. Rather than solving a generic root-finding problem on all intervals and checking all breakpoints, we first analyze the functional form on each piece and identify a set of conditions on the parameters that will lead to a closed-form optimal t_g^*.

Proposition 1. When $\sum_{l:x_{lg}=1} p_l(1-s_l)\left(\frac{\sigma_l}{m_l}\right)^2 \geq \frac{2q}{b+q}$, the optimal time-slot duration for group g is $t_g^* = 0$. When $\frac{2b}{b+q} \leq \sum_{l:x_{lg}=1} p_l \left(\beta_l - \sqrt{S_l(T)} + \frac{\beta_l}{\sqrt{S_l(T)}}\left(\frac{(1+s_l)\sigma_l^2}{2\,\Delta_l^2} - \frac{(1-s_l)\sigma_l^2}{2\,m_l\,\Delta_l}\right)\right)$, where $S_l(T) = \beta_l\left(\beta_l + \frac{(1+s_l)\sigma_l^2}{2\,\Delta_T^2} - \frac{(1-s_l)\sigma_l^2}{m_l\,\Delta_T}\right)$, the optimal time-slot duration for group g is $t_g^* = T$.

Corollary 1. When the unit penalty of overtime vanishes ($q = 0$) or the unit penalty of idle time goes to infinity ($b \to +\infty$), $\sum_{l:x_{lg}=1} p_l(1-s_l)\left(\frac{\sigma_l}{m_l}\right)^2 \geq \frac{2q}{b+q} \to 0$. As a result, setting $t_g^* = 0$ avoids large idle time penalties. On the other hand, when the unit penalty of idle time vanishes ($b = 0$) or the unit penalty of overtime goes to infinity ($q \to +\infty$), $\frac{2b}{b+q} \to 0$ and the condition in Proposition 1 is satisfied. Therefore, the minimum is obtained at $t_g^* = T$ to avoid large overtime penalties.

For non-trivial parameter setups, we provide a road map for finding the closed-form solution t_g^* for group g given the grouping assignment decision $(\boldsymbol{x}, \boldsymbol{y})$ in Algorithm 1. For illustration, consider a toy example with $l = 1, 2$ are assigned to group g and the corresponding parameters satisfying the following relationship

$$
\begin{aligned}
&\tau_1 := 0 < \tau_2 := \frac{m_1}{2} < \tau_3 := \frac{m_2}{2} < \tau_4 := m_1 - \frac{\sigma_1}{2}\sqrt{\frac{1-s_1}{1+s_1}} < \tau_5 := m_2 - \frac{\sigma_2}{2}\sqrt{\frac{1-s_2}{1+s_2}} \\
&\quad < \tau_6 := m_1 + \frac{\sigma_1}{2}\sqrt{\frac{1+s_1}{1-s_1}} < \tau_7 := m_2 + \frac{\sigma_2}{2}\sqrt{\frac{1+s_2}{1-s_2}} < \tau_8 := m_1 + \frac{m_1(1+s_1)}{2(1-s_1)} < \tau_9 := m_2 + \frac{m_2(1+s_2)}{2(1-s_2)}
\end{aligned}
$$

where all the breakpoints partition the feasible region $\mathcal{T}$ into nine disjoint intervals $\mathcal{T}_j = [\tau_j, \tau_{j+1})$, $j = 1, \ldots, 9$ with $\tau_{10} := T$ (see Figure 4).

For group g, we write $\Pi(t_g) = p_1\Pi_1(t_g) + p_2\Pi_2(t_g)$ and substitute the corresponding explicit formulas for $\Pi_1(t_g)$ and $\Pi_2(t_g)$ on each interval $\mathcal{T}_j$ based on Theorem 3. For example, on $\mathcal{T}_1$, both

Algorithm 1: Finding the optimal duration and cost for group g given $(\boldsymbol{x}, \boldsymbol{y})$ and $\rho = 0$.

Input : Grouping assignments $(\boldsymbol{x}, \boldsymbol{y})$, treatment–duration data for group g: $\{(m_l, \sigma_l, s_l), \hat{p}_l\}_{l:x_{lg}=1}$, and cost parameters $b,\ q$.

Construct nominal mode probability $p_l = \frac{x_{lg}\hat{p}_l}{\sum_{l=1}^{L} x_{lg}\hat{p}_l}$ for all $l \in \mathcal{L}$.

Compute intervals $\mathcal{T}_{li}$ for all l such that $x_{lg} = 1$ and $i = 1, \ldots, 5$ following Theorem 3.

All of these intervals $\bigcup_{\substack{l:\, x_{lg}=1 \\ i=1,\ldots,5}} \{\mathcal{T}_{li}\}$ partition the feasible set $\mathcal{T}$ into disjoint intervals $\{\mathcal{T}_j\}_{j=1}^{J}$.

for $j = 1, \ldots, J$ **do**

  Write out $\Pi(t_g) = \sum_{l:x_{lg}=1} p_l \Pi_l(t_g)$ for $t_g \in \mathcal{T}_j$ explicitly based on the closed-form expression of $\Pi_l(t_g)$ in Theorem 3.

  Take the derivative of $\Pi(t_g)$ with respect to t_g on interval $\mathcal{T}_j$, and solve $\frac{\mathrm{d}\Pi(t_g)}{\mathrm{d}t_g} = 0$ to get the root r_{jg}.

  if $r_{jg} \in \mathcal{T}_j$ **then**

    Set $t_g^* = r_{jg}$;

    Break

  else

    Denote the endpoints of interval $\mathcal{T}_j$ as $\{\underline{t}_j, \bar{t}_j\}$;

    Compute $J(\underline{t}_j) = \sum_{l:x_{lg}=1} p_l \Pi_l(\underline{t}_j)$ and $J(\bar{t}_j) = \sum_{l:x_{lg}=1} p_l \Pi_l(\bar{t}_j)$;

    Set $r_{jg} = \arg\min_{t \in \{\underline{t}_j, \bar{t}_j\}} J(t)$;

  end

end

If t_g^* has not been found, then calculate the optimal time-slot duration for group g as $t_g^* = \arg\min_{t_g \in \{r_{jg}\}} \sum_{l:x_{lg}=1} p_l \Pi_l(t_g)$.

Output : Optimal duration t_g^* and optimal cost $\sum_{l:x_{lg}=1} p_l \Pi_l(t_g^*)$ for group g.

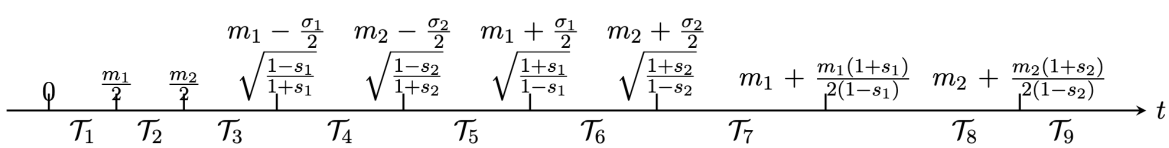

Figure 4: A toy example illustration for $L = 2$.

modes achieve the first linear piece f_{11} and f_{21} and we have $\Pi(t_g) = p_1 f_{11}(t_g) + p_2 f_{21}(t_g)$; on $\mathcal{T}_2$, mode $l = 1$ achieves the second piece f_{12} while mode $l = 2$ still achieves the first linear piece f_{21} and we have $\Pi(t_g) = p_1 f_{12}(t_g) + p_2 f_{21}(t_g)$. We then solve $\frac{d}{dt_g}\Pi(t_g) = 0$ within each $\mathcal{T}_j$ and check if the obtained stationary point is within $\mathcal{T}_j$. If it is true, then we return the stationary point as t_g^* and evaluate $\Pi(t_g^*)$ to obtain the optimal cost for group g. Otherwise, the minimizer is attained at one of the breakpoints. We then evaluate $\Pi_l(t_g)$ at each breakpoint τ_i for $i = 1, \ldots, 10$ and set the one with the smallest cost as t_g^*.

Algorithm 1 returns the optimal time-slot duration t_g^* for each group g given a grouping assignment $(\boldsymbol{x}, \boldsymbol{y})$. Next, we consider the overall problem (1), where the type-to-group assignment is also part of the decisions. We propose Algorithm 2 to find the optimal overall cost by enumerating all possible grouping assignments (i.e., set partitions of the L patient types) and applying Algorithm 1 for each specific grouping assignment.

Algorithm 2: Solving MMA-DRO (9) by enumerating all grouping assignments

---

Input : The moment $m_l,\ \sigma_l,\ s_l$ and $\hat{p}_l$ for each patient type l; cost parameters $b,\ q$.

Put all possible grouping assignments of the L patient types into $\mathcal{P}$.
for *each grouping assignment* $P \in \mathcal{P}$ *with exactly* $|P|$ *groups* **do**
  for $g = 1, \ldots, |P|$ **do**
    Run Algorithm 1 for group g to obtain the optimal duration t_g^* and the optimal cost $\sum_l p_l \Pi_l(t_g^*)$.
  end
  Calculate the overall cost with respect to assignment P:
  $Cost(P) = c_g|P| + \frac{1}{|P|}\sum_{g=1}^{|P|}\sum_{l=1}^{L} p_l \Pi_l(t_g^*)$
end
Select the best grouping assignment $P^* = \arg\min_{P\in\mathcal{P}} Cost(P)$.

Output : optimal overall objective function value $\min_{P\in\mathcal{P}} Cost(P)$, the corresponding assignment decision in P^*, and the optimal time-slot duration for each group.

Specifically, we enumerate all set partitions of the L patient types. For instance, when $L = 3$, this will generate 5 possible grouping assignments, $\{\{1\},\{2\},\{3\}\}, \{\{1,2\},\{3\}\}, \{\{1,3\},\{2\}\}, \{\{2,3\},\{1\}\}$, and $\{1,2,3\}$. Next, for every possible partition, we apply Algorithm 1 on each group g to compute the optimal time-slot duration t_g^* and the optimal cost for group g. We then compute the overall cost for this partition P as $Cost(P)$ by including the assignment cost. Finally, we select partition P that achieves the minimum overall cost. This procedure is exact since it searches all possible partitions of L patient types and is tractable for small L, where the total number of partitions is the Bell number B_L ([28]). The details are outlined in Algorithm 2.

3.2 $\rho > 0$

When $\rho = 0$, the ambiguity set (3) reduces to a singleton, and we leverage the closed-form expression of $\Pi_l(t_g)$ to find the optimal solutions to MMA-DRO model (1) in Section 3.1. However, when we are not confident in the estimated mode probability, we need to set $\rho > 0$. Specifically, Eq. (3) specifies the ambiguity set for the mode probabilities p_l, where the radius ρ controls the allowable deviation between the true mode probabilities p_l and the nominal ones $\hat{p}_l$. In this case, the inner problem also involves the maximization over the ambiguity set $\Delta_g(\hat{\boldsymbol{p}}, \boldsymbol{x}, \boldsymbol{y})$, and we cannot apply Algorithm 1 or 2 to solve it.

Instead, Theorem 2 provides a dual representation of this maximization problem over $\Delta_g(\hat{\boldsymbol{p}}, \boldsymbol{x}, \boldsymbol{y})$, which involves $\Pi_l(t_g)$ on the right-hand side of Eq. (8b). As a result, for a given grouping assignment $(\boldsymbol{x}, \boldsymbol{y})$, we can substitute the closed-form expression of $\Pi_l(t_g)$ into the right-hand side of Eq. (8b) and solve a finite-dimensional convex optimization problem using off-the-shelf solvers, instead of solving the semi-infinite program (9).

Algorithm 3 provides a road map for finding the optimal solutions and the optimal objective value for each group g when $\rho > 0$. Given a grouping assignment $(\boldsymbol{x}, \boldsymbol{y})$, all the intervals $\{T_{lj}\}_{l:x_{lg}=1, j=1,\ldots,5}$,

---

Algorithm 3: Finding the optimal duration and cost for group g given $(\boldsymbol{x}, \boldsymbol{y})$ and $\rho > 0$.

Input : Grouping assignment $(\boldsymbol{x}, \boldsymbol{y})$, treatment–duration data for group g: $\{(m_l, \sigma_l, s_l), p_l\}_{l:x_{lg}=1}$, and cost parameters b, q.

Construct nominal mode probability $p_l = \frac{x_{lg}\hat{p}_l}{\sum_{l=1}^{L} x_{lg}\hat{p}_l}$ for all $l \in \mathcal{L}$.
Compute intervals $\mathcal{T}_{li}$ for all l such that $x_{lg} = 1$ and $i = 1, \ldots, 5$ following Theorem 3.
All of these intervals $\bigcup_{\substack{l:\, x_{lg}=1 \\ i=1,\ldots,5}} \{\mathcal{T}_{li}\}$ partition the feasible set $\mathcal{T}$ into disjoint intervals $\{\mathcal{T}_j\}_{j=1}^{J}$.
for *interval* $\mathcal{T}_j$ $(j = 1, \ldots, J)$, **do**
    Solve $\min_{t_g \in \mathcal{T}_j} \Omega_g(t_g)$, where we replace the right-hand side of Eq. (8b) with the corresponding piece of the function $\Pi_l(t_g)$ with $t_g \in \mathcal{T}_j$ for each $l = 1, \ldots, L$ according to Theorem 2.
    Obtain the optimal time-slot duration t_g^* and optimal cost for group g, $Cost_g(t_g^*)$.
end
Calculate optimal cost overall cost as $\sum_g c_g y_g + \frac{1}{\sum_g y_g} \sum_g Cost_g(t_g^*)$.

Output : Optimal treatment time t_g^* for each group g and optimal overall cost

---

partition the feasible set $\mathcal{T}$ into J intervals $\{\mathcal{T}_j\}_{j=1}^{J}$ and we create J subproblems of (8) by restricting the feasible set for t_g to each T_j. Then in each subproblem, we solve $\min_{t_g \in \mathcal{T}_j} \Omega_g(t_g)$, where we replace the right-hand side of (8b) using the piecewise-convex form from Theorem 3. We then select the overall optimal solution by taking the minimum cost across all J subproblems. This allows us to solve a convex optimization problem each time with finitely many constraints, which is much easier compared to the semi-infinite program (9).

Similar to Algorithm 2, the following algorithm provides an enumeration approach to obtain the grouping assignment and uses Algorithm 3 to obtain the optimal treatment duration t_g^* and the corresponding optimal cost.

Algorithm 4: Solving MMA-DRO (1) by enumerating all grouping assignments

---

Input : The moment m_l, σ_l, s_l for each patient type l; cost parameters b, q.

Put all possible grouping assignments of the L patient types into $\mathcal{P}$.;
for *each grouping assignment* $P \in \mathcal{P}$ *with exactly* $|P|$ *groups* **do**
    for $g = 1, \ldots, |P|$ **do**
        Run Algorithm 3 for group g to obtain the optimal duration t_g^* and the optimal cost $\Omega_g(t_g^*)$.
    end
    Calculate the overall cost with respect to assignment P:
    $Cost(P) = c_g|P| + \frac{1}{|P|} \sum_{g=1}^{|P|} \Omega_g(t_g^*)$
end
Select the best grouping assignment $P^* = \arg\min_{P \in \mathcal{P}} Cost(P)$.

Output : The optimal overall objective function value $\min_{P \in \mathcal{P}} Cost(P)$, the corresponding assignment decision in P^*, and the optimal time-slot duration for each group.

3.3 Lower and Upper Bounds on Each Group's Optimal Cost

To obtain insights into the optimal grouping assignment decisions, we provide lower and upper bounds on each group's optimal cost, which depend on the difference between the maximum and minimum average treatment time among all the patient types assigned to this group. This further sheds light on how to find the optimal grouping assignments: the optimal grouping should group the adjacent types with similar treatment durations (with closer values of m_l), and avoid the clustering of patient types that are distant (with widely different m_l). The proof of the following Propositions 2 and 3 are provided in the Appendices A.7 and A.8, respectively.

We first derive a lower bound of the optimal cost of Problem (10) in the next proposition.

Proposition 2 (Lower bound of Problem (10))**.** For any given group $g \in \mathcal{G}$, define

$$m_{\min}(g) := \min_{l:\, x_{lg}=1} m_l, \qquad m_{\max}(g) := \max_{l:\, x_{lg}=1} m_l,$$

and

$$\overline{p}_{\min}(g) := \max_{\boldsymbol{p}\in\Delta_g(\hat{\boldsymbol{p}},\boldsymbol{x},\boldsymbol{y})} \sum_{\substack{l:\, x_{lg}=1 \\ m_l = m_{\min}(g)}} p_l, \qquad \overline{p}_{\max}(g) := \max_{\boldsymbol{p}\in\Delta_g(\hat{\boldsymbol{p}},\boldsymbol{x},\boldsymbol{y})} \sum_{\substack{l:\, x_{lg}=1 \\ m_l = m_{\max}(g)}} p_l.$$

Then

$$\min_{t_g\in\mathcal{T}} \max_{\boldsymbol{p}\in\Delta_g(\hat{\boldsymbol{p}},\boldsymbol{x},\boldsymbol{y})} \sum_{l:\, x_{lg}=1} p_l\, \Pi_l(t_g) \;\geq\; \frac{b\,\overline{p}_{\min}(g) q\,\overline{p}_{\max}(g)}{b\,\overline{p}_{\min}(g) + q\,\overline{p}_{\max}(g)}(m_{\max}(g) - m_{\min}(g)).$$

In the next proposition, we provide an upper bound of (10), which is also related to the span $m_{\max}(g) - m_{\min}(g)$ for group g.

Proposition 3 (Upper bound of Problem (10))**.** For any group $g \in \mathcal{G}$, define $\sigma_{\max}(g) = \max_{l:x_{lg}=1} \sigma_l$. Then the group-$g$ objective in (10) satisfies

$$\min_{t_g\in\mathcal{T}} \max_{\boldsymbol{p}\in\Delta_g(\hat{\boldsymbol{p}},\boldsymbol{x},\boldsymbol{y})} \sum_{l:x_{lg}=1} p_l \Pi_l(t_g) \leq y_g \max\{b, q\}\Big(\sigma_{\max}(g) + \frac{1}{2}\big(m_{\max}(g) - m_{\min}(g)\big)\Big). \tag{12}$$

From Propositions 2 and 3, both lower and upper bounds of the optimal objective function value of Problem (10) are positively related to the span $m_{\max}(g) - m_{\min}(g)$. This implies that the optimal cost tends to decrease when patient types with similar average treatment times are assigned together. Leveraging this structural insight, we will propose heuristic approaches that cluster patient types according to the similarity of their treatment time statistics in the next section.

4 Heuristic Approaches

In Section 3, we introduced Algorithms 2 and 4, which enumerate all grouping assignments (set partitions) and achieve the global optimum for $\rho = 0$ and $\rho > 0$, respectively. However, such enumeration-based approaches can quickly become computationally inefficient as the number of patient types L grows (the number of possible partitions scales with the Bell number B_L). Motivated by Propositions 2 and 3, in this section, we propose heuristic approaches that leverage clustering algorithms (i.e., K-Means and K-Medoids) to group patient types with similar treatment time statistics, which can produce near-optimal solutions in a quick fashion.

K-Means-based Heuristic. We first use the K-Means method to group patient types based on the similarity of their input feature. Let P_l represent input feature of patient $l \in \mathcal{L}$ (e.g., m_l, σ_l, s_l, or any combination of these moment information). Given the number of activated groups K, our goal is to cluster the L patient types to K groups ($K \leq L$) such that each within-cluster sum of squares objective is minimized. The following problem can be seen as a simplification of Model (1), where we approximate the downstream cost of an assignment by the within-cluster sum of squares. According to Propositions 2 and 3, if the input feature among all the patient types assigned to a group is similar to each other, then it will potentially lead to a lower overall cost.

$$\begin{aligned} \min_{\boldsymbol{x},\boldsymbol{\mu}} \quad & \sum_{l \in \mathcal{L}} \sum_{g=1}^{K} x_{lg} \|P_l - \mu_k\|^2 \\ \text{s.t.} \quad & \sum_{g=1}^{K} x_{lg} = 1, \ \forall l \in \mathcal{L} \\ & x_{lg} \in \{0,1\}, \ \forall l \in \mathcal{L}, \ \forall g = 1, \ldots, K \end{aligned} \tag{13}$$

In Model (13), x_{lg} is the assignment decision as we defined before, and μ_g is the centroid of cluster g. It is non-convex in general because the objective function involves bilinear terms. K-Means algorithm solves (13) by iterating between the following two steps: **(i)** assignment step: given $\boldsymbol{\mu}$, assign each patient type l to its closest cluster $g = \arg\min_g ||P_l - \mu_g||^2$, and **(ii)** update step: given the assignment x^*_{lg}, update the centroids by minimizing the objective in (13) given by $\mu_g = \frac{\sum_{l=1}^{L} x_{lg} P_l}{\sum_{l=1}^{L} x_{lg}}$, $\forall g = 1, \ldots. K$. We iterate between these two steps until assignments stabilize, which yields a local optimum of Problem (13) [7]. The final clusters yield a feasible assignment decision $(\boldsymbol{x}, \boldsymbol{y})$ for our model (10).

Once we obtain a grouping assignment decision $(\boldsymbol{x}, \boldsymbol{y})$, we apply Algorithm 1 and Algorithm 3 to find the optimal duration t^*_g for each group g when $\rho = 0$ and when $\rho > 0$, respectively. To tune the number of activated groups K, we apply cross-validation on the range $K = 1, \ldots, L$ to find the best K that minimizes the average cost on the validation dataset.

K-Medoids-based Heuristic. Different than the K-Means algorithm, where the centroid can fall outside of the input points $\{P_l\}_{l \in \mathcal{L}}$, the K-Medoids algorithm picks a point from the input dataset as a medoid. Specifically, we cluster patient types using K-Medoids on the same feature vectors P_l for $l \in \mathcal{L}$ with a chosen dissimilarity denoted as $\text{dist}(\cdot, \cdot)$. Given the number of activated groups K, we partition L patient types into K clusters by selecting K medoids from the actual data points $\{P_l\}$. Using binary variables $z_i \in \{0,1\}$ to indicate whether type i is selected as a medoid and $r_{li} \in \{0,1\}$ to indicate whether we assign type l to medoid i, the K-Medoids problem is formulated as

$$
\begin{aligned}
\min_{\boldsymbol{r},\boldsymbol{z}} \quad & \sum_{l\in\mathcal{L}}\sum_{i\in\mathcal{L}} r_{li}\,\mathrm{dist}\big(P_l, P_i\big) \\
\text{s.t.} \quad & \sum_{i\in\mathcal{L}} r_{li} = 1,\ \forall\, l \in \mathcal{L}, \\
& r_{li} \le z_i,\ \forall\, l,\ i \in \mathcal{L}, \\
& \sum_{i\in\mathcal{L}} z_i = K, \\
& r_{li},\ z_i \in \{0,1\},\ \forall\, l,\ i \in \mathcal{L}.
\end{aligned} \tag{14}
$$

In the assignment step, given the current medoids $M = \{\, P_i : z_i = 1 \,\}$ (i.e., z_i fixed), for each type l solve (14) to obtain the optimal assignment r^*_{li}, which assigns each l to its nearest medoid. In the update step, given the assignments r^*_{li}, for each cluster g choose the new medoid index and solve for $\boldsymbol{z}$ medoids. Repeat the assignment and update until the objective no longer changes, which yields a local optimum of Problem (14) [32].

K-Means clusters the observations into K groups by iteratively assigning points to the nearest centroid and iteratively updating centroids to minimize the within-cluster sum of squares. By contrast, K-Medoids partitions the observations into K clusters by selecting the representative medoids from the input data points and assigning each observation to its nearest medoid to minimize total within-cluster dissimilarity. Compared with K-Means, K-Medoids is less sensitive to outliers and to skewed or heavy-tailed treatment durations. We will test both methods and compare them with the exact algorithms in Sections 5 and 6.

5 Computational Results based on Synthetic Datasets

In this section, we conduct sensitivity analyses on synthetic datasets and evaluate the in-sample and out-of-sample performance of the exact algorithms (Algorithms 2 and 4) and the heuristics (K-Means and K-Medoids) on these instances.

5.1 Data Generation

We consider the number of patient types L ranging from 5 to 8, and set $G = L$. The group activation cost is set the same across all the groups, i.e., $c_g = 80$. We also set the unit penalty of idle time and overtime as $q = 30,\ b = 20$ at default. The random treatment duration $\tilde{\xi}$ is assumed to have a continuous support $\Xi = [0, 720]$, which covers the 12-hour operational window.

For each mode l, we assume that the treatment time follows a log-normal distribution whose log-mean and log-standard deviation are sampled according to $\mu_l \sim \mathcal{U}(ln(100), ln(600))$ and $\sigma_l \sim \mathcal{U}(0.5, 1.5)$. We draw a nominal mode probability vector $\hat{\boldsymbol{p}} = (\hat{p}_1, \ldots, \hat{p}_L)$ and consider a training dataset of size 100. We then allocate these 100 training data points according to the mode probability and draw $K_l = 100\hat{p}_l$ training samples $\{\xi_{lk}\}_{k=1}^{K_l}$ for each mode l. These samples are then clipped into the $[0, 720]$ range. From the resulting samples, we compute the empirical mean m_l, standard deviation σ_l, and semi-variance s_l for each mode $l \in \mathcal{L}$; these three moments form the input parameters of the MMA-DRO ambiguity set U_l (4). We apply the exact Algorithms 2 and 4 and heuristics (K-Means and K-Medoids) to solve for the grouping assignments $\boldsymbol{x}^*, \boldsymbol{y}^*$, the treatment duration $\boldsymbol{t}^*$, and their corresponding in-sample (IS) costs.

Next, we generate a testing dataset of $1,000$ scenarios by sampling from the same ground-truth log-normal distribution of $\tilde{\xi}$ according to the same nominal mode probability vector $\hat{\boldsymbol{p}}$. We will test the algorithm performance when we perturb the out-of-sample (OOS) distribution in Section 5.3. We evaluate the optimal solutions from solving the MMA-DRO model (1) on the testing dataset to obtain the OOS costs, which allow us to assess the robustness of our algorithms. We report results by averaging over 10 independent runs of this procedure. We also consider the following two benchmarks:

Benchmark I: Sample Average Approximation (SAA). As a benchmark to the MMA-DRO model, we consider an *ambiguity-free* setting where we set $\rho = 0$ to reduce the variation distance set $\Delta_g(\hat{\boldsymbol{p}}, \boldsymbol{x}, \boldsymbol{y})$ to a singleton $\left(\frac{x_{1g}\hat{p}_1}{\sum_{l=1}^{L} x_{lg}\hat{p}_l}, \ldots, \frac{x_{Lg}\hat{p}_L}{\sum_{l=1}^{L} x_{lg}\hat{p}_l}\right)^\mathsf{T}$ and set the ambiguity set U_l to be the empirical distribution $\frac{1}{K_l}\sum_{k=1}^{K_l} \delta_{\xi_{lk}}$, which is supported on the K_l training data points. Under these settings, Model (1) becomes the SAA counterpart.

Benchmark II: Discretized Approximation. As another benchmark, we replace the continuous support set $\xi \in \Xi$ in (9b) with a discrete support $\{0, 1, \ldots, 720\}$, which can be solved by the off-the-shelf solvers (e.g., Gurobi) directly. Because this discretization approximation enforces only a subset of the constraints in Model (9), it provides a valid lower bound to Model (9).

Numerical tests are conducted on a MacBook Pro with 8 GB RAM and an Apple M1 Pro chip. Since the discretized approximation of Model (9) involves non-convex terms, we use Gurobi 10.0.0 coded in Python 3.11.0 for solving all non-convex programming models (with Non-Convex parameter set to 2). The time limit for solving this non-convex program is set to 10 hours.

5.2 Sensitivity Analysis Results

We perform a sensitivity analysis for $L = 5$ and vary the cost parameters b and q, the input feature for the heuristic algorithms, the ambiguity set radius parameter ρ, and the skewness of the log-normal distribution to examine how these parameters affect the overall performance. Summary statistics of both the training and testing datasets are presented in Table 2 below.

Comparison of Different Cost Parameters. We first vary the unit penalty of idle time b from 0 to 30 and vary the unit penalty of overtime q from 20 to 50. The corresponding optimal time-slot durations, IS and OOS costs, and the runtime are reported in Table 3, where we put the patient types assigned to each group in parentheses.

We begin with the default setting, where the overtime cost parameter q is higher than the idle-time cost b to reflect clinical reality in practice. In this case, the optimal assignment is to group

Table 2: Summary statistics for $L = 5$

	Training Data					Testing Data				
Statistic	mode 1	mode 2	mode 3	mode 4	mode 5	mode 1	mode 2	mode 3	mode 4	mode 5
Min	26.64	43.55	32.88	54.98	100.46	21.81	9.92	4.24	20.92	26.76
Max	560.74	720.00	720.00	720.00	720.00	720.00	720.00	720.00	720.00	720.00
Mean	231.58	302.44	366.66	378.14	423.30	276.97	308.72	333.83	353.10	380.01
Std.	170.16	243.91	252.87	248.99	200.03	200.59	257.10	257.25	253.57	229.99
Semi-variance	0.25	0.28	0.16	0.08	0.11	0.36	0.25	0.15	0.14	0.13

Table 3: Comparison of different cost parameters $b,\ q$.

$b,\ q$	Optimal Duration (min.)	IS	OOS			Runtime (sec.)
			Idle time	Overtime	Total cost	
$b = 20,\ q = 30$	$164\ (1),\ 516\ (2,3,4,5)$	5112.99	189.04	72.82	6125.17	0.99
$b = 30,\ q = 20$	$149\ (1),\ 241\ (2,3,4,5)$	4404.14	46.25	154.02	4627.90	1.34
$b = 25,\ q = 25$	$158\ (1),\ 258\ (2,3,4,5)$	4899.70	53.37	145.84	5140.26	0.97
$b = 0,\ q = 50$	$720\ (1,2,3,4,5)$	80	389.95	0	80	0.37
$b = 50,\ q = 0$	$0\ (1,2,3,4,5)$	80	0	329.05	80	0.49

the last four modes, while keeping the first mode a separate group. The second row shows that when the penalty is reversed so that $\frac{b}{q} > 1$, the optimal grouping is unchanged, but the optimal durations decrease, leading to smaller IS and OOS costs. With $\frac{b}{q} < 1$, the model favors longer slots to avoid costly overtime, whereas with $\frac{b}{q} > 1$, idle time is more costly and yields shorter optimal durations. When $\frac{b}{q} = 1$, the optimal durations fall between these two cases.

An extreme setting ($b = 0,\ q = 50$) illustrates this effect better: the model stretches the duration to the maximum value (720 minutes), which yields no idle cost because $b = 0$ nor overtime cost because $(\tilde{\xi} - t_g)^+ = 0$, and the lowest IS cost is obtained when only one group is open. Another extreme setting ($b = 50,\ q = 0$) drives the optimal duration to the minimum value (0 minutes), which yields no overtime cost because $q = 0$ nor idle cost because $(t_g - \tilde{\xi})^+ = 0$. Both agree with our theoretical results in Corollary 1. These observations confirm that the relative magnitudes of b and q govern the trade-off between idle and overtime cost, and therefore shifting the optimal treatment duration t_g^* accordingly.

Comparison of Different Input Features in the Heuristic Algorithms. We compare different input features for the heuristic algorithms (K-Means and K-Medoids) when $\rho = 0$ in this section and present the corresponding results when $\rho = 0.1$ in Appendix B. For each input feature combination, we perform cross-validation (CV) over $k = 1, \ldots, L$ on the training data with $L = 5$ to select the best k. With this k fixed, we run the algorithms to obtain the IS solution $\boldsymbol{t}^*$ and its IS cost. Then we evaluate $\boldsymbol{t}^*$ on the testing dataset to compute the OOS cost. We repeat the entire procedure for 10 independent runs and report the averages in the Tables 4 and 5, for K-Means and K-Medoids algorithms, respectively, where we mark the best IS and OOS costs in bold below.

Tables 4 and 5 show that the feature sets (m_l, s_l) and (m_l, σ_l, s_l) yield the lowest OOS cost

Table 4: Comparison of different input features for K-Means

Feature	IS Cost	OOS Cost	CV Time (sec.)	Solve Time (sec.)	Total Time (sec.)
(m_l, σ_l, s_l)	**4439.88**	4444.85	0.90	0.03	0.93
(m_l)	4448.02	4450.49	0.96	0.04	1.00
(σ_l)	4579.20	4517.30	1.04	0.04	1.08
(s_l)	4537.95	4474.84	0.89	0.04	0.93
(m_l, σ_l)	4469.55	4457.63	0.92	0.03	0.95
(m_l, s_l)	4443.89	**4434.26**	0.90	0.03	0.93
(σ_l, s_l)	4458.68	4465.55	0.89	0.03	0.92

Table 5: Comparison of different input features for K-Medoids

Feature	IS	OOS	CV Time (sec.)	Solve Time (sec.)	Total Time (sec.)
(m_l, σ_l, s_l)	4628.61	**4486.70**	0.56	0.02	0.58
(m_l)	4546.78	4492.57	0.53	0.02	0.55
(σ_l)	**4513.23**	4514.86	0.52	0.02	0.54
(s_l)	4640.32	4511.92	0.53	0.02	0.55
(m_l, σ_l)	4604.95	4495.80	0.50	0.02	0.52
(m_l, s_l)	4559.03	4496.78	0.49	0.02	0.51
(σ_l, s_l)	4557.52	4521.64	0.50	0.02	0.52

for K-Means and K-Medoids-based heuristic algorithms, respectively. Moreover, based on Tables 15 and 16 in Appendix B, for $\rho = 0.1$, K-Means returns the lowest OOS cost using (m_l, s_l), and K-Medoids prefers the full feature set (m_l, σ_l, s_l). These results confirm the managerial insights derived in Section 3.3, which suggest grouping patient types with similar average treatment times. For consistency purposes, we adopt these feature sets for our heuristic algorithms in the remainder of the paper. Furthermore, both heuristic algorithms have a solve time within 0.05 seconds and a CV time of about one second, demonstrating the computational efficiency.

Comparison of Different ρ. We vary the ambiguity set radius ρ over the values $0,\ 0.1,\ 0.5,\ 1$. By construction, $\rho < 1$ because it bounds the total variation distance between the unknown mode probabilities p_l and their nominal references according to (3). The table below reports the average IS costs, OOS costs, and runtime for 10 independent runs.

Table 6: Comparison for different ρ for $L = 5$

ρ	Method	IS	OOS	Runtime (sec.)
0	Algorithm 2	**4031.36**	4659.24	1.69
0.1	Algorithm 4	4071.34	4644.45	1.78
0.5	Algorithm 4	4185.46	**4582.08**	1.56
1	Algorithm 4	4262.82	4683.53	1.46

Table 6 shows that the IS cost rises monotonically with respect to the ambiguity set radius ρ.

When $\rho = 0$, the ambiguity set (3) collapses to the nominal mode probability $p_l = \frac{x_{lg}\hat{p}_l}{\sum_{l=1}^{L} x_{lg}\hat{p}_l}$ for each l. As ρ increases, the ambiguity set (3) enlarges by including more candidate distributions. As a result, the decision maker becomes more conservative, leading to a higher IS cost. As ρ increases, the OOS cost initially decreases, which demonstrates improved robustness to mode probability misspecification. However, when $\rho = 1$, the OOS increases because the ambiguity set admits too many undesired probabilities and therefore is too conservative.

We put the detailed results (the optimal grouping assignments, optimal treatment time-slot durations, IS costs, OOS costs, and runtime) in Appendix C to investigate their changes with respect to ρ for a fixed seed.

Effect of Asymmetry. Next, we investigate the effect of asymmetry in our model. Recall that this asymmetry is captured through the semivariance constraint in the ambiguity set U_l defined in (4). By removing the last semivariance constraint from this set and reformulating the resulting model, we obtain a counterpart, named Multimodal Distributionally Robust Optimization (MM-DRO), which does not consider the asymmetry in the distribution of $\tilde{\xi}$. In this case, the closed-form expression for $\Pi_l(t_g)$ in Theorem 3 does not hold. Therefore, we replace the support set $\xi \in \Xi$ in (9b) with a discrete support $\{0, 1, \ldots, 720\}$ and solve the discretized approximation of MMA-DRO and MM-DRO using Gurobi, respectively.

We adjust the skewness by varying the σ parameter of the log-normal distribution, with a higher σ denoting a higher skewness. We draw from a log-normal distribution with log-mean and log-standard deviation sampled from uniform ranges $\mu_l \sim \mathcal{U}(ln(60), ln(100))$ and $\sigma_l \sim \mathcal{U}(1.5, 2.5)$ at the default setting and change the σ range to examine its impact on the performance. We generate 100 training samples and 1,000 testing samples from this log-normal distribution. We report the average IS cost, OOS cost, and run time for 10 independent runs to compare the performance of both models under varying skewness levels in Table 7.

Table 7: Comparison of different skewness under different models

σ_l	Model	IS	OOS	OOS Gap	Runtime (sec.)
$\mathcal{U}(1.5, 2.5)$	MMA-DRO	**3187.43**	**3625.39**	–	196.21
(Baseline)	MM-DRO	3588.14	3765.48	140.09	314.81
$\mathcal{U}(1.5, 2.5) \times 0.8$	MMA-DRO	**3267.95**	**3537.10**	–	179.25
	MM-DRO	3747.73	3681.34	144.24	398.48
$\mathcal{U}(1.5, 2.5) \times 1.5$	MMA-DRO	**3025.15**	**3509.50**	–	213.44
	MM-DRO	3463.25	3881.54	372.04	235.33
$\mathcal{U}(1.5, 2.5) \times 2$	MMA-DRO	**2872.48**	**3384.79**	–	198.01
	MM-DRO	3277.41	3855.75	470.96	249.08

As shown in Table 7, for a given skewness level, the skew-aware MMA-DRO produces both lower IS and OOS costs than MM-DRO. Moreover, as the log-standard deviation σ increases, the gap of the OOS costs between MMA-DRO and MM-DRO becomes larger. These results highlight that the distributional asymmetry affects both the IS and OOS costs and that ignoring it reduces efficiency and accuracy.

5.3 Performance Comparison between Different Approaches

Model Comparison. We now compare the performance of the exact Algorithm 2, the heuristic algorithms (K-Means and K-Medoids) with their best input features, and the discretized approximation solved by Gurobi when the number of modes L ranges from 5 to 8 in Table 8. When L is small ($L = 5, 6$), we report the results under two discretized approximation benchmarks: **(i)** solving the discretized version of Model (9) by treating $\boldsymbol{y}$ as a decision variable and **(ii)** enumerating all possible grouping assignments $P \in \mathcal{P}$ and solving (9) with $\boldsymbol{y}$ fixed, both of which are solved by Gurobi directly. For the former, the time limit is set to 10 hours; for the latter, we set the time limit for each subproblem with a fixed $\boldsymbol{y}$ to one hour. For larger instances ($L = 7, 8$), we only report the results under the enumeration approach, as treating $\boldsymbol{y}$ as a decision variable is computationally prohibitive within the time limit.

Table 8: Performance comparison across different modes

L	Method	IS	OOS	Runtime (sec.)	Relative error (%)	
					IS	OOS
5	Gurobi + y dec var.	**3997.22**	4684.64	183.48	-0.86	0.54
	Gurobi + enumerate y	**3997.22**	4684.64	247.48	-0.86	0.54
	Algorithm 2	4031.36	4659.24	1.69	–	–
	K-Means	4443.89	**4434.26**	CV: 0.89, Solve: 0.03	10.21	-4.82
	K-Medoids	4628.61	4486.70	CV: 0.51, Solve: 0.02	14.79	-3.70
6	Gurobi + y dec var.	**3808.05**	4830.13	1966.07	-1.79	0.16
	Gurobi + enumerate y	**3808.05**	4830.13	936.17	-1.79	0.16
	Algorithm 2	3877.58	4822.42	5.09	–	–
	K-Means	4373.98	**4606.98**	CV: 1.30, Solve: 0.04	12.80	-4.47
	K-Medoids	4266.21	4633.12	CV: 0.96, Solve: 0.02	10.02	-3.93
7	Gurobi + enumerate y	**3499.36**	4864.61	10996.48 (gap: 1744.44%)	-1.25	0.31
	Algorithm 2	3543.62	4849.74	23.78	–	–
	K-Means	4273.22	4828.71	CV: 1.61, Solve: 0.04	20.58	-0.43
	K-Medoids	4325.10	**4825.83**	CV: 0.98, Solve: 0.02	22.05	-0.49
8	Gurobi + enumerate y	**3638.13**	4811.49	20634.21 (gap: 2943.98%)	-0.74	-0.35
	Algorithm 2	3665.21	4828.39	124.60	–	–
	K-Means	4430.98	**4760.46**	CV: 1.85, Solve: 0.04	20.89	-1.41
	K-Medoids	4555.65	4762.56	CV: 1.21, Solve: 0.03	24.29	-1.36

From Table 8, for smaller instances ($L = 5, 6$), both discretized approximation benchmarks are solved to optimality, which provides a lower bound to Model (9). For larger instances ($L = 7, 8$), the Gurobi solver hits the time limit and returns only the incumbent with a nonzero optimality gap. On the other hand, the exact Algorithm 2 can solve Model (9) to optimality more efficiently. K-Means and K-Medoids, when running with their best input features, produce competitive IS and OOS costs while significantly reducing the runtime. As expected, the heuristic algorithms yield higher IS costs, since clustering does not guarantee optimal grouping assignments, with an IS relative error of 10% $\sim$ 24%. However, the heuristics achieve lower OOS costs with an OOS relative error of -1% $\sim$ -5%. Overall, these clustering-based heuristic approaches are highly efficient, with strong out-of-sample performance on large-scale instances.

Effect of Misspecified Distribution. In the previous sections, we generated the testing data from the same distribution as the training data. We now examine the impact of distributional misspecification of $\tilde{\xi}$. Specifically, for each patient type l, we perturb the log-mean and log-standard deviation by the perturbation parameter ϵ when generating the testing data, i.e.,

$$\mu_l^{\text{mis}} = (1+\epsilon)\,\mu_l \qquad \sigma_l^{\text{mis}} = (1+\epsilon)\,\sigma_l$$

with $\epsilon \in \{0.1, 0.2, 0.3, 0.4, 0.5\}$. To account for the misspecified distribution, we modify the ambiguity set U_l to allow the mean, variance, and semivariance to deviate from the empirical ones within a given radius δ and reformulate the corresponding discretized MMA-DRO$^{\text{mis}}$ model (full details are provided in Appendix D).

We then compare MMA-DRO$^{\text{mis}}$ with its SAA counterpart. Given a fixed $\rho = 0.5$, the OOS cost comparison over 10 independent runs of MMA-DRO$^{\text{mis}}$ and SAA is shown in Figure 5.

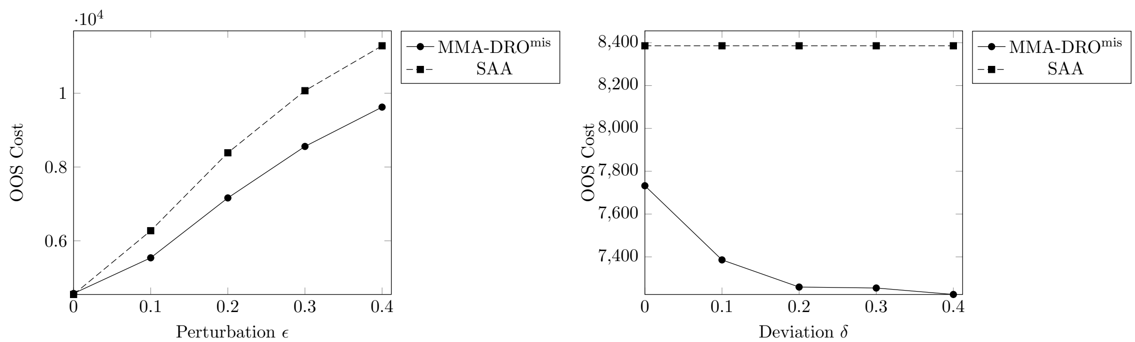

(a) Across perturbation ϵ ($\rho = 0.5$, $\delta = 0.2$).

(b) Across radius δ ($\rho = 0.5$, $\epsilon = 0.2$).

Figure 5: OOS comparisons of MMA-DRO$^{\text{mis}}$ and SAA.

Figure 5a shows that, for a fixed radius ($\delta = 0.2$), the OOS cost increases with the perturbation level ϵ for both models. When $\epsilon = 0$, SAA and MMA-DRO$^{\text{mis}}$ achieve roughly the same OOS cost. However, as ϵ increases, MMA-DRO$^{\text{mis}}$ achieves lower OOS costs compared to SAA, and the performance gap becomes larger. On the other hand, Figure 5b considers a fixed perturbation ($\epsilon = 0.2$) and varies the radius δ in the U_l ambiguity set from 0 to 0.4. As δ increases, the set U_l admits a wider ambiguity in the distributions. Consequently, MMA-DRO$^{\text{mis}}$ attains a lower OOS cost than SAA.

6 Case Study: Mayo Clinic Chemotherapy Dataset

In this section, we evaluate the exact algorithms and proposed heuristics on the Mayo Clinic's real chemotherapy dataset. This dataset contains $1,851$ historical chemotherapy treatment duration records, and each treatment was scheduled into one of the seven predefined time-slot templates (i.e., 30-min, 60-min, etc.). These templates define the seven patient types $l = 1, \dots, L$ in our model with $L = 7$. In this section, we present (i) a comparison between the exact Algorithms 2, 4, the heuristic algorithms K-Means and K-Medoids, and the discretized approximation to solve the MMA-DRO model (9) in Section 6.1; (ii) a comparison across different radii of the mode probability ambiguity set in Section 6.2; (iii) a comparison between the MMA-DRO (1) and its MM-DRO counterpart, which ignores distributional asymmetry in Section 6.3; and (iv) the real-world override comparison in Section 6.4.

6.1 Comparison of Different Models

We apply Algorithm 2, K-Means, K-Medoids, and the discretized approximation solved by Gurobi to compare the optimal treatment durations t_g^* and the corresponding optimal cost. The comparative results are summarized in Table 9.

Table 9: Comparison of Different Algorithms

Method	Optimal Durations (min.)	Optimal Cost	Runtime (sec.)	Relative Error (%)
Gurobi + y dec var.	39, 60, 216	**1268.19**	36000	0
Gurobi + enumerate y	39, 60, 216	1268.19	31682	0
Algorithm 2	39, 60, 216	1268.28	27.16	–
K-Means	58, 118, 217, 368	1409.32	CV: 1.38, Solve: 0.05	11.12
K-Medoids	39, 60, 118, 210, 261, 368	1503.47	CV: 0.91, Solve: 0.04	18.54

For the discretized approximation where we treat $\boldsymbol{y}$ as a decision variable, we set a time limit of 10 hours, within which Gurobi produced the best incumbent solution with a cost of 1268.19 with an optimality gap of 1577116.52%. In contrast, the enumeration method achieved the same overall cost of 1268.19 in 31682 seconds (~ 8.8 hours) with an optimality gap of 481246.74%. The exact Algorithm 2 finds the same optimal assignment $(\boldsymbol{x}^*, \boldsymbol{y}^*)$ decisions and optimal time-slot durations with a cost of 1268.28 more efficiently (within 30 seconds), where the duration $t_1^* = 39$ serves the 30-minute mode, duration $t_2^* = 60$ serves the 60-minute mode, and duration $t_3^* = 216$ jointly accommodates the $\{120, 180, 240, 300, 360\}$-minute modes.

On the other hand, K-Means and K-Medoids both produce near-optimal solutions in roughly two seconds, with the actual solve time around 0.05 seconds. Using this approach, K-Means achieves a cost of 1409.32 with a relative error 11.12% and K-Medoids yields a cost of 1503.47 with a relative error 18.54%. Specifically, K-Means generates four groups with a new time-slot template of $(58, 118, 217, 368)$ minutes ($t_1^* = 58$ to serve the $\{30, 60\}$-minute types, $t_2^* = 118$ to serve the 120-minute type, $t_3^* = 217$ to serve the $\{180, 240, 300\}$-minute types, and $t_4^* = 368$ to serve the 360-minute type, respectively), and K-Medoids yields 6 groups with a new time-slot template of $(39, 60, 118, 210, 261, 368)$ minutes. These results demonstrate that our heuristic algorithms both achieve strong performance while significantly reducing computational time.

Next, we investigate how changing the size of the mode probability ambiguity set $\Delta_g(\hat{\boldsymbol{p}}, \boldsymbol{x}, \boldsymbol{y})$ affects the overall model performance.

6.2 Changing the radius of the ambiguity set ρ

We vary the robustness parameter $\rho \in \{0, 0.1, 0.5, 1\}$ to enlarge the ambiguity set and solve the MMA-DRO model using the exact Algorithms 2 and 4 and the heuristic algorithms. We compare performance between the algorithms and the discretized approximation solved by the Gurobi enumeration method. The comparative results are summarized in Table 10.

Table 10: Comparison for different ρ

ρ	Method	Optimal duration (min.)	Optimal Cost	Runtime (sec.)	Relative Error (%)
0	Gurobi	39, 60, 216	**1268.19**	36000	0
	Algorithm 2	39, 60, 216	1268.28	27.16	–
	K-Means	58, 118, 217, 368	1409.32	CV: 1.38, Solve: 0.05	11.12
	K-Medoids	39, 60, 118, 210, 261, 368	1503.47	CV: 0.91, Solve: 0.04	18.54
0.1	Gurobi	39, 60, 221	**1313.19**	31056	0
	Algorithm 4	39, 60, 221	1313.28	43.65	–
	K-Means	58, 118, 219, 368	1419.94	CV: 2.79, Solve: 0.50	8.12
	K-Medoids	39, 60, 118, 210, 262, 368	1505.64	CV: 2.35, Solve: 0.47	14.62
0.5	Gurobi	39, 60, 218, 368	**1386.86**	33923	0
	Algorithm 4	39, 60, 218, 368	1386.93	41.54	–
	K-Means	59, 118, 225, 368	1456.65	CV: 2.53, Solve: 0.48	5.03
	K-Medoids	39, 60, 118, 210, 278, 368	1512.49	CV: 2.72, Solve: 0.49	9.05
1	Gurobi	39, 60, 238, 368	**1429.12**	39132	0
	Algorithm 4	39, 60, 238, 368	1429.20	41.98	–
	K-Means	60, 118, 238, 368	1486.36	CV: 2.53, Solve: 0.49	3.99
	K-Medoids	39, 60, 118, 210, 280, 368	1512.52	CV: 2.72, Solve: 0.49	5.83

Table 10 shows that the optimal cost increases monotonically with ρ, since a larger ambiguity set admits more adversarial mode probabilities, making the inner maximization problem to have higher costs and leading to more conservative decisions. For example, from $\rho = 0.5$ to $\rho = 1$, the grouping of the 7 patient types remains unchanged, but the inner maximization shifts probability mass toward longer-duration modes, raising the optimal durations t_3^* (e.g., the third group's duration increases from 218 to 238). Also, from $\rho = 0.1$ to $\rho = 0.5$, Algorithm 4 opens a fourth group to trade additional assignment cost for reduced overtime by isolating the 360-minute mode. This result also illustrates how increasing the size of the ambiguity set ρ values drives more conservative solutions.

We also observe that, the optimal costs returned by the exact Algorithms 2 and 4 are upper bounds on those from the discretized approximation solved by Gurobi, since the latter enforces only a subset of constraints. Moreover, both K-Means and K-Medoids algorithms perform well, achieving relative errors approximately between 4% and 15% while substantially reducing the computational time.

6.3 Effect of Asymmetry

As described previously, once we remove the last equality constraint from the U_l ambiguity set in (4), an exact algorithm is no longer available. Therefore, we compare solutions from solving the discretized approximation model under two specifications: explicitly modeling the distributional asymmetry, and omitting it. We compare the optimal decisions t_g^*, the corresponding optimal cost, and the run time in Table 11.

Table 11: Effect of Asymmetry Comparison

Model	Optimal Durations (min.)	Optimal Cost	Runtime (sec.)	Relative Error (%)
MMA-DRO	39, 60, 216	**1268.19**	31682 (gap: 1577116.52%)	–
MM-DRO	55, 81, 217	1448.63	36000 (gap: 1136385.25%)	14.23

Table 11 shows that omitting the asymmetry by removing the semivariance constraint from the ambiguity set U_l causes the optimal cost to increase by 14.23% compared to the original MMA-DRO model. This gap demonstrates the value of including the asymmetry information that better hedges against the skewness in treatment duration distributions.

6.4 Real-world Override Comparison between the Optimized Template and the Current Template

In chemotherapy scheduling, an override occurs when the allocated slots in a daily template are insufficient to accommodate the realized number of patients in a given category. This typically arises when patients call to schedule appointments, and the hospital operator assigns them to the most appropriate available time slot in the daily template. If no suitable slot exists within the same category as the patient type, the operator may split a longer slot or merge two shorter ones, resulting in an override.

Following the Mayo Clinic's current practice, we evaluate the number of overrides by calculating the difference between the allocated number of time slots and the realized number of patient counts in each patient type based on a three-month validation dataset. Specifically, Mayo Clinic's current daily template contains 79 time slots for 19 chairs in total, having a capacity of 8,970 minutes. Recall that the optimal time-slot durations produced by Algorithm 2 in Table 9 are 39, 60, and 216 minutes to accommodate the 30-min, 60-min, and $120, 180, 240, 300, 360$-min patient types, respectively. Using the same capacity, we allocate the 8,970 minutes to the three patient groups according to the percentage of these groups shown in the one-month training dataset, resulting in $(25, 14, 33)$ slots for $(39, 60, 216)$ minutes, respectively. Then, on the three-month validation set, we compare the allocated time slots with the realized counts for each patient group on each day. When the template allocates fewer slots than the realized demand, we record an override. We apply the same procedure to Mayo Clinic's current template to compute its override counts.

Table 12 compares override counts between Mayo Clinic's current template and the optimized template, where the last row calculates the total duration, number of time slots, and number of overrides, respectively. The current template has a total of 37 overrides, whereas the new template

Table 12: Comparison of overrides under the current and new templates.

(a) Current template for 19 chairs

	Duration (min.)	Slots	Overrides
	30	27	2
	60	17	0
	120	11	4
	180	10	27
	240	7	3
	300	3	1
	360	4	0
Total	8,970	79	37

(b) New template generated by MMA-DRO

	Duration (min.)	Slots	Overrides
	39	25	15
	60	14	2
	216	33	0
Total	8,970	72	17

only has 17 overrides, representing a 54% reduction in overrides. This decrease indicates that reallocating slots based on solving the MMA-DRO model (1) achieves a better alignment between planned capacity and realized durations.

7 Conclusion

In this paper, we developed a multimodal asymmetric DRO (MMA-DRO) model for chemotherapy template design that jointly determines the patient-type-to-grouping assignments and the corresponding optimal time-slot durations for each group. The ambiguity set captured both multi-modality across patient types and asymmetry in treatment-duration distributions. To handle the intractability of the resulting semi-infinite program, we proposed **(i)** exact algorithms that enumerate all possible grouping assignments and solve for an optimal duration for each group based on the closed-form expression of the inner maximization problem; **(ii)** heuristics that first cluster patient types via K-Means and K-Medoids to obtain the grouping assignments and then solve for the time-slot duration for each group; and **(iii)** a discretized approximation solved by off-the-shelf solvers, in which the continuous support is replaced by a discrete support.

We evaluated the performance of the above algorithms on synthetic datasets and the Mayo Clinic's real chemotherapy dataset. Compared with the discretized approximation solved by Gurobi, our exact algorithms achieved optimality much more efficiently, and the heuristic approaches (K-Means and K-Medoids) yielded competitive IS and OOS costs while substantially reducing runtime on large instances. Sensitivity analyses further suggested that as the radius of the ambiguity set grows, the IS cost produced by the exact algorithms increases monotonically, whereas the OOS cost tends to decrease, indicating an improved robustness to distribution misspecification. Compared with the asymmetry-unaware counterpart MM-DRO, MMA–DRO consistently outperforms MM–DRO, which highlights the value of explicitly modeling asymmetry. We observed similar insights on the Mayo Clinic's real dataset. Furthermore, the optimized template generated by our MMA-DRO model significantly reduced overrides compared to the Mayo Clinic's current template. In future work, we will extend our optimization framework to optimize the placement of time slots in a daily template that explicitly minimizes the downstream overrides. This paper mainly considered moment-based ambiguity sets to capture distributional uncertainty. We will also consider distance-based ambiguity sets to incorporate the asymmetric information in the underlying treatment distributions.

References

[1] Alvarado, M. and Ntaimo, L. (2018). Chemotherapy appointment scheduling under uncertainty using mean-risk stochastic integer programming. *Health care management science*, 21(1):87–104.

[2] Bansal, A., Berg, B., and Huang, Y.-L. (2021). A distributionally robust optimization approach for coordinating clinical and surgical appointments. *IISE transactions*, 53(12):1311–1323.

[3] Bauerhenne, C., Kolisch, R., and Schulz, A. S. (2024). Robust appointment scheduling with waiting time guarantees. *arXiv preprint arXiv:2402.12561*.

[4] Bayraksan, G. and Love, D. K. (2015). Data-driven stochastic programming using phi-divergences. In *The operations research revolution*, pages 1–19. Informs.

[5] Behnamian, J. and Gharabaghli, Z. (2023). Multi-objective outpatient scheduling in health centers considering resource constraints and service quality: a robust optimization approach. *Journal of Combinatorial Optimization*, 45(2):80.

[6] Blanchet, J. and Murthy, K. (2019). Quantifying distributional model risk via optimal transport. *Mathematics of Operations Research*, 44(2):565–600.

[7] Bottou, L. and Bengio, Y. (1994). Convergence properties of the k-means algorithms. *Advances in neural information processing systems*, 7.

[8] Castaing, J., Cohn, A., Denton, B. T., and Weizer, A. (2016). A stochastic programming approach to reduce patient wait times and overtime in an outpatient infusion center. *IIE Transactions on Healthcare Systems Engineering*, 6(3):111–125.

[9] Chen, H., He, Y., QI, J., and Zhang, L. (2023). Distributionally robust pricing with asymmetric information. *Available at SSRN 4365395*.

[10] Chen, L., Fu, C., Si, F., Sim, M., and Xiong, P. (2024). Robust optimization with moment-dispersion ambiguity. *Operations Research*.

[11] Chen, X., Sim, M., and Sun, P. (2007). A robust optimization perspective on stochastic programming. *Operations research*, 55(6):1058–1071.

[12] Delage, E. and Ye, Y. (2010). Distributionally robust optimization under moment uncertainty with application to data-driven problems. *Operations research*, 58(3):595–612.

[13] Demir, N. B., Gul, S., and Çelik, M. (2021). A stochastic programming approach for chemotherapy appointment scheduling. *Naval Research Logistics (NRL)*, 68(1):112–133.

[14] Esfahani, P. M. and Kuhn, D. (2018). Data-driven distributionally robust optimization using the wasserstein metric: Performance guarantees and tractable reformulations. *Mathematical Programming*, 171(1-2):115–166.

[15] Gao, R. and Kleywegt, A. (2023). Distributionally robust stochastic optimization with wasserstein distance. *Mathematics of Operations Research*, 48(2):603–655.

[16] Gul, S. (2021). Chemotherapy appointment scheduling under uncertainty by considering workload balance among nurses. *Pamukkale Üniversitesi Mühendislik Bilimleri Dergisi*, 27(4):570–578.

[17] Hanasusanto, G. A., Kuhn, D., Wallace, S. W., and Zymler, S. (2015). Distributionally robust multi-item newsvendor problems with multimodal demand distributions. *Mathematical Programming*, 152(1):1–32.

[18] Hristov, S. (2025). *Distributionally Robust Chance Constraints for Radiotherapy Treatment Planning under Geometric Uncertainty*. PhD thesis, University of Waterloo.

[19] Huang, Y.-L., Bach, S. M., and Looker, S. A. (2019). Chemotherapy scheduling template development using an optimization approach. *International journal of health care quality assurance*, 32(1):59–70.

[20] Huang, Y.-L., Bryce, A. H., Culbertson, T., Connor, S. L., Looker, S. A., Altman, K. M., Collins, J. G., Stellner, W., McWilliams, R. R., Moreno-Aspitia, A., et al. (2018). Alternative outpatient chemotherapy scheduling method to improve patient service quality and nurse satisfaction. *Journal of oncology practice*, 14(2):e82–e91.

[21] Isii, K. (1962). On sharpness of tchebycheff-type inequalities. *Annals of the Institute of Statistical Mathematics*, 14(1):185–197.

[22] Issabakhsh, M., Lee, S., and Kang, H. (2021). Scheduling patient appointment in an infusion center: a mixed integer robust optimization approach. *Health Care Management Science*, 24:117–139.

[23] Jiang, R. and Guan, Y. (2016). Data-driven chance constrained stochastic program. *Mathematical Programming*, 158(1-2):291–327.

[24] Jiang, R. and Guan, Y. (2018). Risk-averse two-stage stochastic program with distributional ambiguity. *Operations Research*, 66(5):1390–1405.

[25] Karakaya, S., Gul, S., and Çelik, M. (2023). Stochastic scheduling of chemotherapy appointments considering patient acuity levels. *European Journal of Operational Research*, 305(2):902–916.

[26] Keyvanshokooh, E., Kazemian, P., Fattahi, M., and Van Oyen, M. P. (2022). Coordinated and priority-based surgical care: An integrated distributionally robust stochastic optimization approach. *Production and Operations Management*, 31(4):1510–1535.

[27] Mehrotra, S. and Papp, D. (2014). A cutting surface algorithm for semi-infinite convex programming with an application to moment robust optimization. *SIAM Journal on Optimization*, 24(4):1670–1697.

[28] Mezo, I. (2011). The r-bell numbers. *J. Integer Seq*, 14(1):1–14.

[29] Natarajan, K., Pachamanova, D., and Sim, M. (2008). Incorporating asymmetric distributional information in robust value-at-risk optimization. *Management Science*, 54(3):573–585.

[30] Natarajan, K., Sim, M., and Uichanco, J. (2018). Asymmetry and ambiguity in newsvendor models. *Management Science*, 64(7):3146–3167.

[31] Sagawa, S., Koh, P. W., Hashimoto, T. B., and Liang, P. (2019). Distributionally robust neural networks for group shifts: On the importance of regularization for worst-case generalization. *arXiv preprint arXiv:1911.08731*.

[32] Schubert, E. and Rousseeuw, P. J. (2019). Faster k-medoids clustering: improving the pam, clara, and clarans algorithms. In *International conference on similarity search and applications*, pages 171–187. Springer.

[33] Shehadeh, K. S., Cohn, A. E., and Jiang, R. (2020). A distributionally robust optimization approach for outpatient colonoscopy scheduling. *European Journal of Operational Research*, 283(2):549–561.

[34] Shehadeh, K. S. and Sanci, E. (2021). Distributionally robust facility location with bimodal random demand. *Computers & Operations Research*, 134:105257.

[35] Wagner, M. R. (2008). Stochastic 0–1 linear programming under limited distributional information. *Operations Research Letters*, 36(2):150–156.

[36] Yu, X. and Basciftci, B. (2024). Distributionally robust optimization with multimodal decision-dependent ambiguity sets.

[37] Yu, X. and Shen, S. (2022). Multistage distributionally robust mixed-integer programming with decision-dependent moment-based ambiguity sets. *Mathematical Programming*, 196(1):1025–1064.

[38] Zhang, Y., Jiang, R., and Shen, S. (2018). Ambiguous chance-constrained binary programs under mean-covariance information. *SIAM Journal on Optimization*, 28(4):2922–2944.

A Omitted Proofs

A.1 Proof for Theorem 1

Proof. We first expand the ambiguity set by writing out all moment constraints in U_l as follows

$$\Pi_l(t_g) = \quad \max_{f_l} \int_{\tilde{\xi} \in \Xi} f_l(\tilde{\xi}) \left(q(\tilde{\xi} - t_g)^+ + b(t_g - \tilde{\xi})^+ \right)$$

$$
\begin{aligned}
\text{s.t.} \quad & \int_{\tilde{\xi}\in\Xi} f_l(\tilde{\xi})\, d\tilde{\xi} = 1, \\
& \int_{\tilde{\xi}\in\Xi} \tilde{\xi} f_l(\tilde{\xi})\, d\tilde{\xi} = m_l, \\
& \int_{\tilde{\xi}\in\Xi} (\tilde{\xi} - m_l)^2 f_l(\tilde{\xi})\, d\tilde{\xi} = \sigma_l^2, \\
& \int_{\tilde{\xi}\in\Xi} f_l(\tilde{\xi})(\tilde{\xi} - m_l)^{+2}\, d\tilde{\xi} - \int_{\tilde{\xi}\in\Xi} f_l(\tilde{\xi})(m_l - \tilde{\xi})^{+2}\, d\tilde{\xi} = s_l\sigma_l^2, \\
& f_l(\tilde{\xi}) \geq 0,\ \forall \tilde{\xi} \in \Xi.
\end{aligned} \tag{15}
$$

Since any feasible t_g is bounded and Ξ is a compact set, the objective function of (15) is bounded. Furthermore, according to Proposition 2.1 in [30], Assumption 1 guarantees that the ambiguity set U_l is nonempty. Following Theorem 1 in [21], strong duality holds. Assigning dual variables $\gamma_{lg},\ \nu_{lg},\ \kappa_{lg},\ \zeta_{lg}$ to constraints in (15), the dual formulation of (15) can then be written as

$$
\begin{aligned}
\Pi_l(t_g) = \min_{\gamma_{lg},\nu_{lg},\kappa_{lg},\zeta_{lg}} \quad & \gamma_{lg} + \nu_{lg} m_l + \kappa_{lg}\sigma_l^2 + \zeta_{lg} s_l \sigma_l^2 \\
\text{s.t.} \quad & \gamma_{lg} + \nu_{lg}\tilde{\xi} + \kappa_{lg}(\tilde{\xi} - m_l)^2 + \zeta_{lg}\left((\tilde{\xi} - m_l)^{+2} - (m_l - \tilde{\xi})^{+2}\right) \\
& \geq q(\tilde{\xi} - t_g)^+ + b(t_g - \tilde{\xi})^+,\ \forall \tilde{\xi} \in \Xi \\
& \gamma_{lg},\ \nu_{lg},\ \kappa_{lg},\ \zeta_{lg} \in \mathbb{R}.
\end{aligned}
$$

This completes the proof. □

A.2 Proof for Theorem 2

Proof. Expand $\Omega_g(t_g)$ under the ambiguity set $\Delta_g(\hat{\boldsymbol{p}}, \boldsymbol{x}, \boldsymbol{y})$ defined in (3) as follows

$$
\begin{aligned}
\max_{p_l} \quad & \sum_{l=1}^{L} p_l \Pi_l(t_g) \\
\text{s.t} \quad & \sum_{l=1}^{L} p_l = y_g, && \text{(16a)} \\
& 0 \leq p_l \leq x_{lg},\ \forall l \in \mathcal{L}, && \text{(16b)} \\
& \sum_{l=1}^{L} \left| p_l \Big(\sum_{l=1}^{L} x_{lg}\hat{p}_l \Big) - x_{lg}\hat{p}_l \right| \leq \rho \sum_{l=1}^{L} x_{lg}\hat{p}_l. && \text{(16c)}
\end{aligned}
$$

We have shown that $\Pi_l(t_g)$ is bounded in Theorem 1 under Assumption 1. Moreover, for any feasible $(\boldsymbol{x}, \boldsymbol{y}, \boldsymbol{t})$, we can always find a feasible $\boldsymbol{p}$ that satisfies Problem (16). For instance, if group g is not activated ($y_g = 0$), then no patient type is assigned to this group ($x_{lg} = 0,\ \forall l \in \mathcal{L}$). As a result, $\boldsymbol{p} = (0, \ldots, 0)^\top$ is a feasible solution to Problem (16). If group g is activated ($y_g = 1$), then at least one patient type is assigned to group g. As a result, simply setting $p_l = \frac{x_{lg}\hat{p}_l}{\sum_{l=1}^{L} x_{lg}\hat{p}_l}$ for all $l \in \mathcal{L}$ yields a feasible solution.

To formulate the dual, we first linearize the absolute value term in Constraint (16c) by introducing an auxiliary nonnegative variable d_{lg} as

$$d_{lg} \geq p_l\Big(\sum_{l=1}^{L} x_{lg}\hat{p}_l\Big) - x_{lg}\hat{p}_l, \tag{17a}$$

$$d_{lg} \geq x_{lg}\hat{p}_l - p_l\Big(\sum_{l=1}^{L} x_{lg}\hat{p}_l\Big), \tag{17b}$$

$$\sum_{l=1}^{L} d_{lg} \leq \rho \sum_{l=1}^{L} x_{lg}\hat{p}_l, \tag{17c}$$

$$d_{lg} \geq 0. \tag{17d}$$

Replacing Constraint (16c) with Constraints (17a)–(17d), we obtain a linear programming (LP) formulation of the primal problem (16). Assigning dual variables μ_g, λ_{lg}, α_{lg}, β_{lg}, and τ_g to Constraint (16a), (16b), (17a), (17b), and (17c), respectively, we derive the dual formulation of Problem (16) for group g as follows

$$\begin{aligned}
\min_{\mu_g,\lambda_{lg},\tau_g,\alpha_l,\beta_l} \quad & \mu_g y_g + \sum_{l=1}^{L} \lambda_{lg} x_{lg} + \sum_{l=1}^{L} (\alpha_{lg} - \beta_{lg})\hat{p}_l x_{lg} + \rho\tau_g \sum_{l=1}^{L} x_{lg}\hat{p}_l \\
\text{s.t.} \quad & \mu_g + \lambda_{lg} + (\alpha_{lg} - \beta_{lg})(\sum_{l=1}^{L} x_{lg}\hat{p}_l) \geq \Pi_l(t_g), \ \forall l \in \mathcal{L} \\
& -\alpha_{lg} - \beta_{lg} + \tau_g \geq 0, \ \forall l \in \mathcal{L} \\
& \mu_g \in \mathbb{R}, \ \lambda_{lg}, \ \alpha_{lg}, \ \beta_{lg}, \ \tau_g \geq 0.
\end{aligned}$$

Since this LP is feasible and bounded, we obtain the strong duality. □

A.3 Proof for Theorem 3

Proof. To reformulate problem (6), we first rewrite the U_l ambiguity as follows (7) as

$$\begin{aligned}
& \max_{f_l} \int_{\tilde{\xi}\in\Xi} f_l(\tilde{\xi}) \left(q(\tilde{\xi} - t_g)^+ + b(t_g - \tilde{\xi})^+ \right) \\
\text{s.t.} \quad & \int_{\tilde{\xi}\in\Xi} f_l(\tilde{\xi})\, d\tilde{\xi} = 1, \\
& \int_{\tilde{\xi}\in\Xi} (\tilde{\xi} - m_l)^+ f_l(\tilde{\xi}) d\tilde{\xi} - \int_{\tilde{\xi}\in\Xi} (m_l - \tilde{\xi})^+ f_l(\tilde{\xi}) d\tilde{\xi} = 0, \\
& \int_{\tilde{\xi}\in\Xi} f_l(\tilde{\xi})(\tilde{\xi} - m_l)^{+2}\, d\tilde{\xi} = \frac{(1+s_l)\sigma_l^2}{2}, \\
& \int_{\tilde{\xi}\in\Xi} f_l(\tilde{\xi})(m_l - \tilde{\xi})^{+2}\, d\tilde{\xi} = \frac{(1-s_l)\sigma_l^2}{2}, \\
& f_l(\tilde{\xi}) \geq 0, \ \forall \tilde{\xi} \geq 0.
\end{aligned} \tag{18}$$

Assign dual variables $\alpha,\ \beta,\ y_1$ and y_2 to derive the dual formulation of (18) to be

$$\begin{aligned}
\min_{\alpha,\beta,y_1,y_2} \quad & \beta + \frac{(1+s_l)\sigma_l^2}{2} y_1 + \frac{(1-s_l)\sigma_l^2}{2} y_2 \\
\text{s.t} \quad & \beta + \alpha(x-m_l) + y_1(x-m_l)^2 \geq q(x-t_g)^+ + b(t_g-x)^+,\ \forall x \geq m_l \\
& \beta + \alpha(x-m_l) + y_2(x-m_l)^2 \geq q(x-t_g)^+ + b(t_g-x)^+,\ \forall 0 \leq x < m_l
\end{aligned} \tag{19}$$

The goal is to construct primal and dual feasible solutions with the same objective values and obtain optimal solutions. Let $f_1(x),\ g_1(x),\ f_2(x)$, and $g_2(x)$ denote the LHS and RHS of the first and second constraint, respectively. Let $w_1,\ w_2$ denote $\frac{(1+s_l)\sigma_l^2}{2},\ \frac{(1-s_l)\sigma_l^2}{2}$, respectively. Checking feasibility is equivalent to verifying $f_1(x) \leq g_1(x)$ for all $x \geq m_l$, and $f_2(x) \leq g_2(x)$ for all $0 \leq x \leq m_l$, where the equalities are satisfied when the primal distribution has positive masses. The optimal cost is obtained by evaluating either the optimal primal or the optimal dual solution on its respective objective function.

Case 1. Suppose $m_l > t_g$. In this case, $g_1(x) = q(x-t_g)$ and

$$g_2(x) = \begin{cases} q(x-t_g), & t_g \leq x < m_l, \\ b(t_g - x), & 0 \leq x < t_g \end{cases}$$

(1*a*) Let $f_1(x)$ coincide with $g_1(x)$ for all $x \geq m_l$. Then on this domain we have

$$\beta + \alpha(x-m_\ell) + y_1(x-m_\ell)^2 = q(x-t_g).$$

Since f_1 is linear in this region, we set $y_1 = 0$. Then the matching coefficients are $\alpha = q,\ \beta = q(m_l - t_g)$. Let $f_2(x)$ intersect with $g_2(x)$ on $x_1 = 0$ (See Figure 6a). Then we can get $y_2 = \frac{(b+q)t_g}{m_l^2}$.

Since f_1 and g_1 coincide on infinitely many, but an unknown number of points, the primal distribution must consist of at least two support points. Suppose it is a two-point distribution. Denote x_1 to be the x-coordinate of the unique intersection of f_1 and g_1. Then the two-point primal distribution is

$$\tilde{\xi} = \begin{cases} 0, \text{ w.p. } p_1 \\ x_2, \text{ w.p. } p_2, \end{cases}$$

which does not satisfy the primal feasibility condition in Eq. (18).

Consequently, denote $x_2 > m_l,\ x_3 > m_l$ to be the x-coordinates of the two intersection points and consider the following three-point distribution

$$\tilde{\xi} = \begin{cases} 0, \text{ w.p. } p_1 \\ x_2, \text{ w.p. } p_2 \\ x_3, \text{ w.p. } p_3, \end{cases}$$

and substitute it into Eq. (18). Since the system of equations contains five unknowns $(x_2,\ x_3,\ p_1,\ p_2,\ p_3)$ and only four equalities, we introduce a parameter π and express each variable in terms of π. As a result, this three-point primal distribution is

$$\tilde{\xi} = \begin{cases} 0 & \text{w.p.} \frac{w_2}{m^2} \\ \frac{m_l}{m^2 - w_2}(m^2 - \sqrt{w_1(m^2 - w_2) - w_2^2}\sqrt{\frac{1-\pi}{\pi}}) & \text{w.p.} \pi(1 - \frac{w_2}{m^2}) \\ \frac{m_l}{m^2 - w_2}(m^2 + \sqrt{w_1(m^2 - w_2) - w_2^2}\sqrt{\frac{\pi}{1-\pi}}) & \text{w.p.} (1-\pi)(1 - \frac{w_2}{m^2}) \end{cases} \tag{20}$$

with $\pi \in \left[1 - \frac{w_2^2}{w_1(m_l^2 - w_2)}, 1\right)$. t_g lies in the interval $[0, \frac{m_l}{2})$, ensuring that $f_2'(0) > -b$.

$(1b)$ Assume $f_1(x)$ coincide with $g_1(x)$ for all $x \geq m_l$. We have $y_1 = 0,\ \alpha = q$, and $\beta = q(m_l - t_g)$ from the previous. Now let $f_2(x)$ be tangent to $g_2(x)$ on $x \in (0, m_l)$ (See Figure 6b). Let x_1 denote the x-coordinate of the tangent point x^*, we can write out the system of equations for $f_2(x)$ and $g_2(x)$ as

$$\begin{cases} qm_l - qt_g - q(m - x_1) + y_2(m - x_1)^2 = b(t - x_1) \\ 2y_2(x_1 - m) + q = -b \\ 0 \leq x_1 \leq t_g \end{cases} \tag{21}$$

Solving this equation gives us $x_1 = 2t_g - m_l,\ y_2 = \frac{b+q}{4(m_l - t_g)}$.

Suppose it is a two-point distribution. Let $x_2 \geq m_l$ denote the x-coordinate of the unique intersection point of f_1 and g_1. Then we can write

$$\tilde{\xi} = \begin{cases} 2t_g - m_l, \text{w.p. } p_1 \\ x_2, \text{w.p. } p_2, \end{cases}$$

which does not satisfy the primal feasibility condition in Eq. (18).

Consequently, denote $x_2 > m_l,\ x_3 > m_l$ to be the x-coordinates of the two intersection points and consider the following three-point distribution

$$\tilde{\xi} = \begin{cases} 2t_g - m_l,\ \text{w.p. } p_1 \\ x_2,\ \text{w.p. } p_2 \\ x_3,\ \text{w.p. } p_3 \end{cases}$$

and substitute it into Eq. (18). Using a similar approach and introducing the variable π, this three-point primal distribution is

$$\tilde{\xi} = \begin{cases} 2t_g - m_l & \text{w.p.} \frac{w_2}{(2m_l - 2t_g)^2} \\ m_l + \frac{2(m_l - t_g)}{4(m_l - t_g)^2 - w_2}(w_2 - \sqrt{4w_1(m_l - t_g)^2 - w_2(w_1 + w_2)}\sqrt{\frac{1-\pi}{\pi}}) & \text{w.p.} \pi(1 - \frac{w_2}{(2m_l - 2t_g)^2}) \\ m_l + \frac{2(m_l - t_g)}{4(m_l - t_g)^2 - w_2}(w_2 + \sqrt{4w_1(m_l - t_g)^2 - w_2(w_1 + w_2)}\sqrt{\frac{\pi}{1-\pi}}) & \text{w.p.} (1 - \pi)(1 - \frac{w_2}{(2m_l - 2t_g)^2}) \end{cases}$$

with $\pi \in [1 - \frac{w_2^2}{w_1[4(m - t_g)^2 - w_2]}, 1)$. t_g lies in the interval $[\frac{m_l}{2}, m_l - \frac{1}{2}\sqrt{\frac{w_2(w_1 + w_2)}{w_1}})$, ensuring that $f_2(0) \geq g_2(0)$.

(1c) Let $f_1(x)$ be tangent to $g_1(x)$ at x_1 and $f_2(x)$ be tangent to $g_2(x)$ at x_2, where $x_1 \geq m_l$, $0 \leq x_2 \leq t_g$ and $y_1, y_2 > 0$ (See Figure 6c). Then the primal admits a two–point distribution

$$\tilde{\xi} = \begin{cases} x_1, & \text{w.p } p_1 \\ x_2, & \text{w.p } p_2 \end{cases}$$

Substituting into Eq. (18) yields the system

$$\begin{cases} \beta + \alpha(x_1 - m_l) + y_1(x_1 - m_l)^2 = q(x_1 - t_g) \\ 2y_1(x_1 - m_l) + \alpha = q \\ \beta + \alpha(x_2 - m_l) + y_2(x_2 - m_l)^2 = b(t_g - x_2) \\ 2y_2(x_2 - m_l) + \alpha = -b \end{cases} \tag{22}$$

which contains four variables and two equations. This system involves four variables and only two equations. Introducing a parameter π and setting $p_2 = \pi$, $p_1 = 1 - \pi$ then substituting into Eq. (22) gives $\pi = \frac{w_1}{w_1 + w_2}$. Hence, the optimal primal distribution is

$$\tilde{\xi} = \begin{cases} m_l + \sqrt{\frac{w_1(w_1 + w_2)}{w_2}} & \text{w.p.} \frac{w_2}{w_1 + w_2} \\ m_l - \sqrt{\frac{w_2(w_1 + w_2)}{w_1}} & \text{w.p.} \frac{w_1}{w_1 + w_2} \end{cases} \tag{23}$$

Substituting this back into Eq. (22), we obtain the dual optimal solution

$$\begin{cases} \beta = \frac{(m_l - t_g)(qw_2 - bw_1)}{w_1 + w_2} + \frac{b+q}{2}\sqrt{\frac{w_1 w_2}{w_1 + w_2}}, \\ \alpha = q - \frac{b+q}{w_1 + w_2}[2(t_g - m_l)\sqrt{\frac{w_1 w_2}{w_1 + w_2}} - w_2], \\ y_1 = \frac{w_2(t_g - m_l)(b+q)}{(w_1 + w_2)^2} + \frac{b+q}{2}\frac{w_2}{w_1 + w_2}\frac{w_2}{w_1(w_1 + w_2)}, \\ y_2 = \frac{w_1(m_l - t_g)(b+q)}{(w_1 + w_2)^2} + \frac{b+q}{2}\frac{w_1}{w_1 + w_2}\frac{w_1}{w_2(w_1 + w_2)}, \end{cases}$$

and t_g lies in the interval $[m_l - \frac{1}{2}\sqrt{\frac{w_2(w_1 + w_2)}{w_1}}, , m_l)$, ensuring that y_1, $y_2 > 0$.

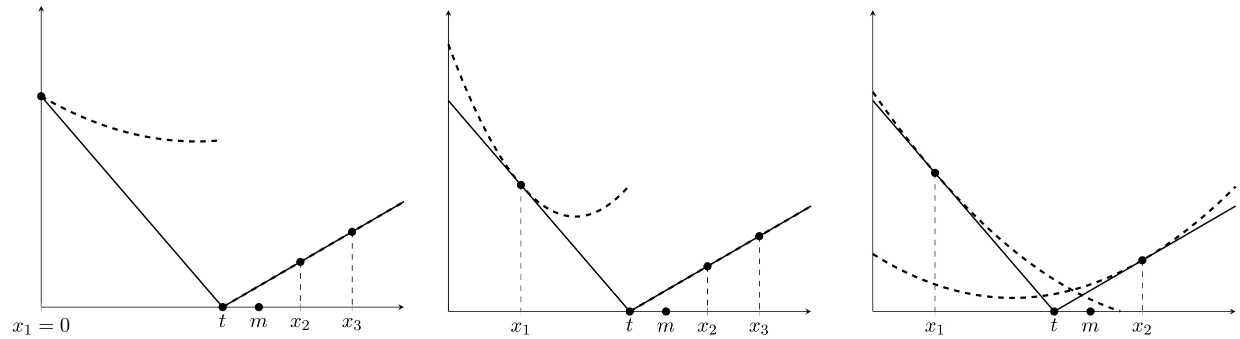

(a) Case 1a (b) Case 1b (c) Case 1c

Figure 6: Case 1 $m_l \geq t_g$ illustrations

Case 2. Suppose $m_l \leq t_g$. In this case, $g_2(x) = q(x - t_g)$ and

$$g_1(x) = \begin{cases} q(x - t_g), & x \geq t_g \\ b(t_g - x), & m_l < x \leq t_g \end{cases}$$

$(2a)$ Assume f_2 coincide with g_2 on $[0, m_l)$. On this domain, we have

$$\beta + \alpha(x - m_l) + y_2(x - m_l)^2 = b(t_g - x).$$

Since f_2 is linear in this region, we set $y_2 = 0$. Then the matching coefficients are $\alpha = -b$, $\beta = bt_g - bm_l$. Let f_1 be tangent to g_1 on $x_1 > t_g$, where x_1 denotes the x-coordinate of the tangent point. In this case, we obtain the system of equations

$$\begin{cases} bt_g - bm_l - b(x_1 - m_l) + y_1(x_1 - m_l)^2 = q(x_1 - t_g) \\ 2y_1(x_1 - m_l) - b = q \end{cases}$$

Solving for $y_1 = \frac{b+q}{4(t_g - m_l)}$ and $x_1 = 2t_g - m_l$. Similar to case $(1b)$, we know that the primal optimal distribution $\tilde{\xi}$ is a three-point distribution

$$\tilde{\xi} = \begin{cases} 2t_g - m_l & \text{w.p.} \frac{w_1}{(2m_l - 2t)^2} \\ m_l - \frac{2(t_g - m_l)}{4(t_g - m_l)^2 - w_1}\left(w_1 - \sqrt{4w_2(t_g - m_l)^2 - w_1(w_1 + w_2)}\sqrt{\frac{1-\pi}{\pi}}\right) & \text{w.p.} \pi\left(1 - \frac{w_1}{(2m_l - 2t_g)^2}\right) \\ m_l - \frac{2(t_g - m_l)}{4(t_g - m_l)^2 - w_1}\left(w_1 + \sqrt{4w_2(t_g - m_l)^2 - w_1(w_1 + w_2)}\sqrt{\frac{\pi}{1-\pi}}\right) & \text{w.p.} (1 - \pi)\left(1 - \frac{w_1}{(2m_l - 2t_g)^2}\right), \end{cases}$$

with the auxiliary variable $\pi \in \left[1 - \frac{w_2^2}{w_1(4(m_l - t_g)^2 - w_2)}, 1\right)$. t_g lies in the interval $\left[m_l + \frac{1}{2}\sqrt{\frac{w_2(w_1 + w_2)}{w_1}}, m_l + \frac{m_l w_1}{2w_2}\right)$ ensuring that $x_2 > x_3$ and that the square root expressions are well defined.

(2b) Assume f_1 is tangent to g_1 on $x_1 > t_g$ and f_2 is tangent to g_2 on $x_2 \in [0, m_l)$, where $x_1,\ x_2$ are the x-coordinates of the tangent points. In this case, we obtain the system of equations

$$\begin{cases} \beta + \alpha(x_1 - m_l) + y_1(x_1 - m_l)^2 = q(x_1 - t_g) \\ 2y_1(x_1 - m_l) + \alpha = q \\ \beta + \alpha(x_2 - m_l) + y_2(x_2 - m_l)^2 = b(t_g - x_2) \\ 2y_2(x_2 - m_l) + \alpha = -b, \end{cases}$$

with the corresponding two-point primal optimal distribution

$$\tilde{\xi} = \begin{cases} x_1,\ \text{w.p. } p_1 \\ x_2,\ \text{w.p. } p_2. \end{cases}$$

This is exactly the same as case (1c). Solving for variables $(x_1,\ x_2,\ p_1,\ p_2,\ y_1,\ y_2,\ \alpha,\ \beta)$, we obtain the same result. t_g lies in the interval of $\left[m_l, m_l + \frac{1}{2}\sqrt{\frac{w_2(w_1+w_2)}{w_1}}\right)$ ensuring $y_1,\ y_2 > 0$.

(2c) Let f_2 be concave and intersect with g_2 at $x_1 = 0$, where x_1 is the x-coordinate of the intersection point. Let f_1 be tangent to g_1 at $m_l \le x_2 < t_g$ and $x_3 \ge t_g$, where $x_2,\ x_3$ are the x-coordinates of the two tangent points. In this case, the primal optimal distribution is a three-point distribution

$$\tilde{\xi} = \begin{cases} 0,\ \text{w.p. } p_1 \\ x_2,\ \text{w.p. } p_2 \\ x_3,\ \text{w.p. } p_3, \end{cases}$$

and the system of equations is

$$\begin{cases} \beta - \alpha m_l + y_2 m_l^2 = b t_g \\ \beta + \alpha(x_2 - m_l) + y_1(x_2 - m_l)^2 = b(t_g - x_2) \\ 2y_1(x_2 - m_l) + \alpha = -b \\ \beta + \alpha(x_3 - m_l) + y_1(x_3 - m_l)^2 = q(x_3 - t_g) \\ 2y_1(x_3 - m_l) + \alpha = q \end{cases}$$

Together with the primal feasibility condition (18), we obtain nine equations in nine variables, which return a unique solution for the primal optimal distribution and the corresponding optimal dual solutions. t_g^* lies in the range of $[m_l + \frac{m_l w_1}{2w_2}, \infty)$ ensuring the concavity of f_1.

Case 1. $m_l \ge t_g$ In this case, $g_1(x) = q(x - t_g)$, $g_2(x) = q(x - t_g)$ for $t_g \le x \le m_l$, and $b(t_g - x)$ for $0 \le x \le t_g$.

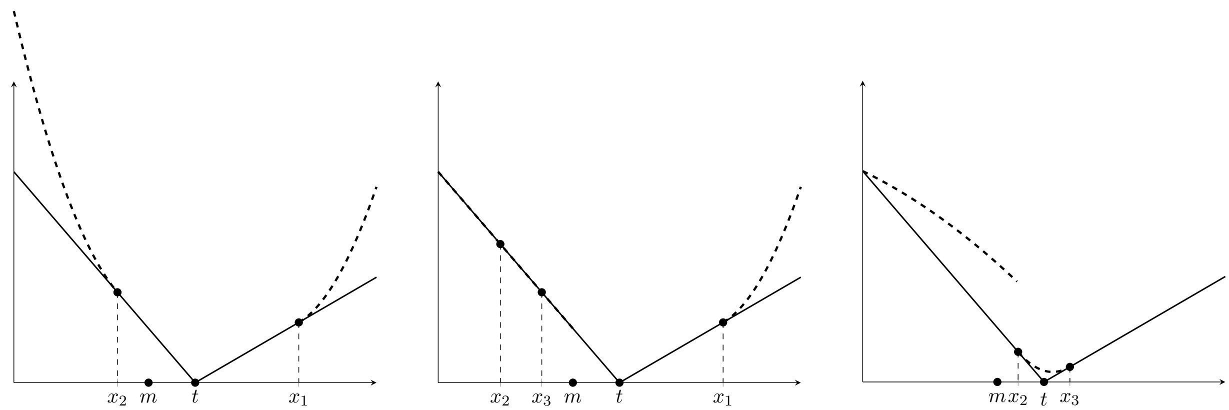

(a) Case 2a (b) Case 2b (c) Case 2c

Figure 7: Case 2 $m_l \leq t_g$ illustrations

Case 2. $m_l < t_g$ In this case, $g_2(x) = b(t_g - x)$, and $g_1(x) = b(t_g - x)$ for $m_l \leq x \leq t_g$, and $q(x - t_g)$ for $x \geq t_g$. □

A.4 Proof for Theorem 4

Proof. First, Problem (10) becomes a convex problem since the objective function $\Pi(t_g) = \sum_{l=1}^{L} p_l \, \Pi_l(t_g)$ is a convex combination of convex functions and is therefore convex in t_g. By the optimality condition for convex programs with a box constraint $\mathcal{T} = [0, T]$, $t_g^* \in \arg\min_{t_g \in \mathcal{T}} \Pi(t_g)$ if and only if $0 \in \partial_{t_g} \Pi(t_g^*) + \mathcal{N}_{\mathcal{T}}(t_g^*)$, where the normal cone of $\mathcal{T}$ is defined as follows

$$\mathcal{N}_{\mathcal{T}}(t_g) = \begin{cases} \{0\}, & t_g \in (0, T), \\ (-\infty, 0], & t_g = 0, \\ [0, \infty), & t_g = T. \end{cases}$$

Because each piece $f_{li}(t_g)$ is differentiable on its interval $\mathcal{T}_{li}$ for each mode $l = 1, \ldots, L$ and $i = 1, \ldots, 5$, $\Pi(t_g)$ is also differentiable on each of the intervals $\mathcal{T}_j$ for $j = 1, \ldots, J$. If there exists $t_g^* \in int(\mathcal{T}_j)$ that satisfies $\sum_{l:\, x_{lg}=1} p_l \, \Pi_l'(t_g^*) = 0$ (i.e., a stationary point of a convex function piece), then at this point, $\mathcal{N}_{\mathcal{T}}(t_g^*) = \{0\}$ and $0 \in \partial_{t_g} \Pi(t_g^*) + \mathcal{N}_{\mathcal{T}}(t_g^*)$. As a result, t_g^* is optimal. If no such interior point exists on any $\mathcal{T}_j$, the minimizer must be attained at an endpoint of the intervals, i.e., $t_g^* = 0$ if the one-sided gradient $\nabla_{t_g} \Pi(0) \geq 0$, $t_g = T$ if the one-sided gradient $\nabla_{t_g} \Pi(T) \leq 0$, and t_g^* is achieved at an endpoint other than 0 and T if $0 \in \partial_{t_g} \Pi(t_g^*)$.

□

A.5 Proof for Proposition 1

Proof. Recall that MMA-DRO (1) is convex in t_g. Since $\Pi(t_g) = \sum_{l:x_{lg}=1} p_l \Pi_l(t_g)$ is bounded and convex for group $g \in \mathcal{G}$, the optimizer is determined by **(i)** the sign of the slope on the linear pieces and **(ii)** whether the nonlinear pieces admit interior stationary points.

Case 1(a): $0 \le t_g \le \frac{m_l}{2}$. Primal feasible distribution: $\tilde{\xi} = \begin{cases} 0 & \text{w.p.} \frac{w_2}{m^2} \\ \frac{m_l}{m^2-w_2}(m^2 - \sqrt{w_1(m^2-w_2)-w_2^2}\sqrt{\frac{1-\pi}{\pi}}) & \text{w.p.}\pi(1-\frac{w_2}{m^2}) \\ \frac{m_l}{m^2-w_2}(m^2 + \sqrt{w_1(m^2-w_2)-w_2^2}\sqrt{\frac{\pi}{1-\pi}}) & \text{w.p.}(1-\pi)(1-\frac{w_2}{m^2}) \end{cases}$ where $\pi \in \left[1 - \frac{w_2^2}{w_1(m_l^2-w_2)}, 1\right)$. Dual feasible solution: $\beta = qm_l - qt_g,\ \alpha = q,\ y_1 = 0,\ y_2 = \frac{(b+q)t_g}{m_l^2}$. Optimal Cost: $qm_l - qt_g + w_2\frac{(b+q)t_g}{m_l^2} = (\frac{(b+q)(1-s_l)\sigma_l^2}{2m_l^2} - q)t_g + qm_l$.
Case 1(b): $\frac{m_l}{2} \le t_g \le m_l - \frac{1}{2}\sqrt{\frac{w_2(w_1+w_2)}{w_1}}$. Primal feasible distribution: $\tilde{\xi} = \begin{cases} 2t_g - m_l & \text{w.p.} \frac{w_2}{(2m_l-2t_g)^2} \\ m_l + \frac{2(m_l-t_g)}{4(m_l-t_g)^2-w_2}(w_2 - \sqrt{4w_1(m_l-t_g)^2 - w_2(w_1+w_2)}\sqrt{\frac{1-\pi}{\pi}}) & \text{w.p.}\pi(1-\frac{w_2}{(2m_l-2t_g)^2}) \\ m_l + \frac{2(m_l-t_g)}{4(m_l-t_g)^2-w_2}(w_2 + \sqrt{4w_1(m_l-t_g)^2 - w_2(w_1+w_2)}\sqrt{\frac{\pi}{1-\pi}}) & \text{w.p.}(1-\pi)(1-\frac{w_2}{(2m_l-2t_g)^2}) \end{cases}$ where $\pi \in [1 - \frac{w_2^2}{w_1[4(m-t_g)^2-w_2]}, 1)$. Dual feasible solution: $\beta = qm_l - qt_g,\ \alpha = q,\ y_1 = 0,\ y_2 = \frac{(b+q)}{4(m_l-t_g)}$. Optimal Cost: $qm_l - qt_g + w_2\frac{b+q}{4(m_l-t_g)} = \frac{(b+q)(1-s_l)\sigma_l^2}{8(m_l-t_g)} - qt_g + qm_l$.
Case 1(c): $m_l - \frac{1}{2}\sqrt{\frac{w_2(w_1+w_2)}{w_1}} \le t_g \le m_l$. Primal feasible distribution: $\tilde{\xi} = \begin{cases} m_l + \sqrt{\frac{w_1(w_1+w_2)}{w_2}} & \text{w.p.} \frac{w_2}{w_1+w_2} \\ m_l - \sqrt{\frac{w_2(w_1+w_2)}{w_1}} & \text{w.p.} \frac{w_1}{w_1+w_2} \end{cases}$ Dual feasible solution: $\beta = \frac{(m_l-t_g)(qw_2-bw_1)}{w_1+w_2} + \frac{b+q}{2}\sqrt{\frac{w_1w_2}{w_1+w_2}}$, $\alpha = q - \frac{b+q}{w_1+w_2}[2(t_g-m_l)\sqrt{\frac{w_1w_2}{w_1+w_2}} - w_2]$, $y_1 = \frac{w_2(t_g-m_l)(b+q)}{(w_1+w_2)^2} + \frac{b+q}{2}\frac{w_2}{w_1+w_2}\frac{w_2}{w_1(w_1+w_2)}$, $y_2 = \frac{w_1(m_l-t_g)(b+q)}{(w_1+w_2)^2} + \frac{b+q}{2}\frac{w_1}{w_1+w_2}\frac{w_1}{w_2(w_1+w_2)}$, Optimal Cost: $(b+q)\sqrt{\frac{w_1w_2}{w_1+w_2}} + (m_l-t_g)\frac{qw_2-bw_1}{w_1+w_2} = \frac{(b+q)\sigma_l}{2}\sqrt{1-s_l^2} + (m_l-t_g)\frac{(q-b)-(q+b)s_l}{2}$.

Table 13: Primal and dual optimal solution when $m_l \ge t_g$

1. *Initial decrease on $\mathcal{T}_1$ (first piece).* Define the common first-piece domain $\mathcal{T}_1 := \bigcap_{l:\, x_{lg}=1} \mathcal{T}_{l1} = \left[0, \min_{l:\, x_{lg}=1} \frac{m_l}{2}\right]$. On $\mathcal{T}_1$, we have

$$\Pi(t_g) = \sum_{l:\, x_{lg}=1} p_l\, f_{l1}(t_g) = \Big(\sum_{l:\, x_{lg}=1} p_l\, k_l\Big)\, t_g \; + q \sum_{l:\, x_{lg}=1} p_l m_l,$$

Case 2(a) $m_l \le t_g \le m_l + \frac{1}{2}\sqrt{\frac{w_2(w_1+w_2)}{w_1}}$. Primal feasible distribution: $\tilde{\xi} = \begin{cases} m_l + \sqrt{\frac{w_1(w_1+w_2)}{w_2}} & \text{w.p.} \frac{w_2}{w_1+w_2} \\ m_l - \sqrt{\frac{w_2(w_1+w_2)}{w_1}} & \text{w.p.} \frac{w_1}{w_1+w_2} \end{cases}$ Dual feasible solution: $\beta = \frac{(m_l-t_g)(qw_2-bw_1)}{w_1+w_2} + \frac{b+q}{2}\sqrt{\frac{w_1w_2}{w_1+w_2}}$, $\alpha = q - \frac{b+q}{w_1+w_2}[2(t_g-m_l)\sqrt{\frac{w_1w_2}{w_1+w_2}} - w_2]$, $y_1 = \frac{w_2(t_g-m_l)(b+q)}{(w_1+w_2)^2} + \frac{b+q}{2}\frac{w_2}{w_1+w_2}\frac{w_2}{w_1(w_1+w_2)}$, $y_2 = \frac{w_1(m_l-t_g)(b+q)}{(w_1+w_2)^2} + \frac{b+q}{2}\frac{w_1}{w_1+w_2}\frac{w_1}{w_2(w_1+w_2)}$, Optimal Cost: $(b+q)\sqrt{\frac{w_1w_2}{w_1+w_2}} + (t_g-m_l)\frac{bw_1-qw_2}{w_1+w_2} = \frac{(b+q)\sigma_l}{2}\sqrt{1-s_l^2} + (m_l-t_g)\frac{(q-b)-(q+b)s_l}{2}$.
Case 2(b): $m_l + \frac{1}{2}\sqrt{\frac{w_2(w_1+w_2)}{w_1}} \le t_g \le m_l + \frac{m_l w_1}{2w_2}$ Primal feasible distribution: $\tilde{\xi} = \begin{cases} 2t_g - m_l & \text{w.p.} \frac{w_1}{(2m_l-2t)^2} \\ m_l - \frac{2(t_g-m_l)}{4(t_g-m_l)^2-w_1}(w_1 - \sqrt{4w_2(t_g-m_l)^2 - w_1(w_1+w_2)}\sqrt{\frac{1-\pi}{\pi}}) & \text{w.p.} \pi(1-\frac{w_1}{(2m_l-2t_g)^2}) \\ m_l - \frac{2(t_g-m_l)}{4(t_g-m_l)^2-w_1}(w_1 + \sqrt{4w_2(t_g-m_l)^2 - w_1(w_1+w_2)}\sqrt{\frac{\pi}{1-\pi}}) & \text{w.p.} (1-\pi)(1-\frac{w_1}{(2m_l-2t_g)^2}) \end{cases}$ where $\pi \in \left[1 - \frac{w_2^2}{w_1(4(m_l-t_g)^2-w_2)}, 1\right)$. Dual feasible solution: $\beta = bt_g - bm_l,\ \alpha = -b,\ y_1 = \frac{(b+q)}{4(t_g-m_l)},\ y_2 = 0$ Optimal Cost: $bt_g - bm_l + w_1\frac{b+q}{4(t_g-m_l)} = \frac{(b+q)(1+s_l)\sigma_l^2}{8(t_g-m_l)} + bt_g - bm_l$.
Case 2(c) $m_l + \frac{m_l w_1}{2w_2} \le t_g$. Primal feasible distribution: $\tilde{\xi} = \begin{cases} 0 & \text{w.p.} \frac{w_2}{m_l^2} \\ t_g - \sqrt{\frac{(t_g-m_l)^2(m_l^2-w_2)+m_l^2w_1-2m_lw_2(t_g-m_l)}{m_l^2-w_2}} & \text{w.p.} 1 - \frac{w_2}{m_l^2} - \frac{w_2^2}{m_l^2 w_1} \\ t_g + \sqrt{\frac{(t_g-m_l)^2(m_l^2-w_2)+m_l^2w_1-2m_lw_2(t_g-m_l)}{m_l^2-w_2}} & \text{w.p.} \frac{w_2^2}{m^2 w_1} \end{cases}$ Dual feasible solution: $\beta = \frac{t_g-m_l}{2}\left[\left(q-3b\right)\sqrt{\frac{2A+B}{B}} - 3(b+q)\sqrt{\frac{B}{2A+B}} - \left(6b+4q\right)\right]$ $\alpha = b + (b+q)\sqrt{\frac{B}{2A+B}}$, $y_1 = \frac{b+q}{2(t_g-m_l)}\sqrt{\frac{B}{2A+B}}$, $y_2 = \frac{1}{2m_l^2}\left[4\left(t_g(2b+q) - m_l(b+q)\right) + (m_l-t_g)(q-3b)\sqrt{\frac{2A+B}{B}} + (3t_g-m_l)(b+q)\sqrt{\frac{B}{2A+B}}\right]$ where $A := \frac{w_1}{2(t_g-m_l)^2} - \frac{w_2}{m_l(t_g-m)},\ B = 1 - \frac{w_2}{m_l^2}$ Optimal Cost: $bt_g + qm_l - \frac{b+q}{2}(m_l + (1-\frac{w_2}{m_l^2})t_g - (t_g-m_l)\sqrt{(1-\frac{w_2}{m_l^2})((1-\frac{w_2}{m_l^2}) + \frac{m_lw_1-2w_2(t_g-m_l)}{m_l(t_g-m_l)^2})})$.

Table 14: Primal and dual optimal solution when $m_l \le t$

which is linear in t_g with $k_l := \frac{(b+q)(1-s_l)\sigma_l^2}{2m_l^2} - q$. Therefore, the gradient of $\Pi(t_g)$ on $\mathcal{T}_1$ is

$$\sum_{l:x_{lg}=1} p_l k_l = \sum_{l:x_{lg}=1} p_l\left(\frac{(b+q)(1-s_l)\sigma_l^2}{2m_l^2} - q\right).$$

When $\sum_{l:x_{lg}=1} p_l(1-s_l)\left(\frac{\sigma_l}{m_l}\right)^2 \geq \frac{2q}{b+q}$, then the objective function $\Pi(t_g)$ is nondecreasing in t_g for $t_g \in \mathcal{T}_1$. Because $\Pi(t_g)$ is convex in t_g, it must be nondecreasing for all other pieces. As a result, the global minimizer is attained at the left endpoint of $\mathcal{T}_1$, i.e., $t_g^* = 0$.

2. *Last decrease on $\mathcal{T}_5$ (last piece).* Define the common last-piece domain $\mathcal{T}_5 := \bigcap_{l:\, x_{lg}=1} \mathcal{T}_{l5} = \left[\max_{l:x_{lg}=1} m_l + \frac{m_l(1+s_l)}{2(1-s_l)}, T\right]$. On $\mathcal{T}_5$, we have

$$\Pi(t) = \sum_{l:\, x_{lg}=1} p_l\, f_{l5}^{(l)}(t_g), \quad \text{and } \partial\Pi(t_g) \;=\; \sum_{l:\, x_{lg}=1} p_l\, \partial f_{l5}(t_g).$$

The subgradients of $\Pi(t_g)$ are monotone nondecreasing in t_g when $t_g \in \mathcal{T}_5$. Since $\partial\Pi(t_g) \in \left[\Pi'_-(t_g), \Pi'_+(t_g)\right]$, and the largest subgradient is attained at the right endpoint T.

$$\sup_{t_g \in \mathcal{T}_5} \Pi'_+(t_g) = \Pi'_+(T^-) \leq 0$$

Denote $\Delta_{t_g,l} = t_g - m_l > 0$. Differentiating f_{l5} with respect to t_g and evaluate at T gives:

$$f'_{l5,+}(T^-) = b - \frac{b+q}{2}\left[\beta_l - \sqrt{S_l(T)} + \frac{\beta_l}{\sqrt{S_l(T)}}\left(\frac{(1+s_l)\sigma_l^2}{2\,\Delta_{T,l}^2} - \frac{(1-s_l)\sigma_l^2}{2\,m_l\,\Delta_{T,l}}\right)\right],$$

where $S_l(T) = \beta_l\left(\beta_l + \frac{(1+s_l)\sigma_l^2}{2\,\Delta_{T,l}^2} - \frac{(1-s_l)\sigma_l^2}{m_l\,\Delta_{T,l}}\right)$. Consequently, $\Pi(t_g)$ is nonincreasing on $\mathcal{T}_5$ iff $\sum_{l:x_{lg}=1} p_l f'_{l5,+}(T^-) \leq 0$, i.e.

$$\sum_{l:x_{lg}=1} p_l b - \sum_{l:x_{lg}=1} p_l \frac{b+q}{2}\left[\beta_l - \sqrt{S_l(T)} + \frac{\beta_l}{\sqrt{S_l(T)}}\left(\frac{(1+s_l)\sigma_l^2}{2\,\Delta_{T,l}^2} - \frac{(1-s_l)\sigma_l^2}{2\,m_l\,\Delta_{T,l}}\right)\right] \;\leq\; 0. \tag{24}$$

Denote $H_l(T) := \;\beta_l - \sqrt{S_l(T)} + \frac{\beta_l}{\sqrt{S_l(T)}}\left(\frac{(1+s_l)\sigma_l^2}{2\,\Delta_l^2} - \frac{(1-s_l)\sigma_l^2}{2\,m_l\,\Delta_l}\right)$. Then Eq. (24) is equivalent to

$$\frac{2b}{b+q} \leq \sum_{l:x_{lg}=1} p_l H_l(T) \tag{25}$$

This completes the proof. □

A.6 Proof for Corollary 1

Proof. From Proposition 1, we know

$$\sum_{l:\, x_{lg}=1} p_l(1-s_l)\left(\frac{\sigma_l}{m_l}\right)^2 \;\geq\; \frac{2q}{b+q} \quad\Longrightarrow\quad t_g^* = 0,$$

and

$$\sum_{l:\, x_{lg}=1} p_l H_l(T) \;\geq\; \frac{2b}{b+q} \quad \Longrightarrow \quad t_g^* = T.$$

When $q = 0$ or $b \to +\infty$, $\frac{2q}{b+q} \to 0$ and $\sum_{l:\, x_{lg}=1} p_l(1-s_l)\left(\frac{\sigma_l}{m_l}\right)^2$ is always nonnegative under Assumption 1. As a result, the model chooses $t_g^* = 0$ to be the optimal solution.

Now we show $H_l(T) \geq 0$. Under the Assumption 1, $\beta_l > 0$. Denote $\Delta = T - m_l$ and

$$A_l(\Delta) := \frac{w_{1l}}{\Delta_{l,T}^2} - \frac{2w_{2l}}{m_l \Delta_{l,T}}, \qquad B_l(\Delta) := \frac{w_{1l}}{\Delta_{l,T}^2} - \frac{w_{2l}}{m_l \Delta_{l,T}},$$

and we can write $S_l(T) = \beta_l\big(\beta_l + A_l(\Delta)\big)$.

Furthermore, on $\mathcal{T}_5$, we have $\Delta \geq m_l + \frac{m_l(1+s_l)}{2(1-s_l)} - m_l = \frac{m_l(1+s_l)}{2(1-s_l)} := \Delta_l^{\min}$. Since $A_l(\Delta_l^{\min}) = \frac{2\sigma_l^2(1-s_l)^2}{m_l^2(1+s_l)} - \frac{2\sigma_l^2(1-s_l)^2}{m_l^2(1+s_l)} = 0$ and $A_l'(\Delta) < 0$ (nonincreasing), obtaining the minimum value $A_l(\Delta^*) = -\frac{(1-s_l)^2\sigma_l^2}{2(1+s_l)m_l^2}$ at $\Delta^* = \frac{m_l(1+s_1)}{1-s_l} = 2\Delta_l^{\min}$. Therefore,

$$\beta_l + A_l(\Delta) \geq \beta_l - \frac{(1-s_l)^2\sigma_l^2}{2(1+s_l)m_l^2} = 1 - \frac{(1-s_l)\sigma_l^2}{m_l^2(1+s_l)} \geq 0$$

under the Assumption 1. As a result, $S_l(T) \geq 0$.

Based on the analysis, we can get

$$S_l(T) = \beta_l\big(\beta_l + A_l(\Delta)\big) \leq \beta_l^2 \quad \Rightarrow \quad \sqrt{S_l(T)} \leq \beta_l.$$

Multiplying $H_l(T)$ by $\sqrt{S_l(T)} > 0$ and using $S_l(T) = \beta_l(\beta_l + A_l(\Delta)$ we have

$$\begin{aligned} H_l(T) \geq 0 \iff & \beta_l\sqrt{S_l(T)} - S_l(T) + \beta_l B_l(\Delta) \;\geq\; 0 \\ \iff & \sqrt{S_l(T)} - (\beta_l + A_l(\Delta)) + B_l(\Delta) \;\geq\; 0 \\ \iff & B_l(T) \;\geq\; (\beta_l + A_l(\Delta)) - \sqrt{S_l(T)}. \end{aligned}$$

Since $A_l(\Delta) \leq 0$ and $\sqrt{S_l(T)} \leq \beta_l$,

$$(\beta_l + A_l(\Delta)) - \sqrt{S_l(T)} \;\geq\; (\beta_l + A_l(\Delta)) - \beta_l \;=\; A_l(\Delta).$$

As a result, it suffices to show $B_l(\Delta) \geq A_l(\Delta)$. Notice that

$$B_l(\Delta) - A_l(\Delta) = \frac{w_{2l}}{m_l \Delta_{l,T}} \;\geq\; 0,$$

since all w_{2l}, m_l, and $\Delta_{l,T}$ are all nonnegative, which indicates $H_l(T) \geq 0$ for all $t_g \in \mathcal{T}_5$.

Therefore, Eq. (25) can be satisfied as $q \to +\infty$ or $b = 0$, which both drive $\frac{2b}{b+q}$ to 0 and in such cases, $t_g^* = T$ is optimal.

□

A.7 Proof for Proposition 2

Proof. For any $t_g \in [0,T]$, denote $\phi_{t_g}(\tilde{\xi}) \triangleq q(\tilde{\xi}-t_g)^+ + b(t_g-\tilde{\xi})^+$, which is convex in $\tilde{\xi}$. By Jensen's inequality, we have

$$\Pi_l(t_g) = \max_{f_l\in U_l} \mathbb{E}_{f_l}\big[\phi_{t_g}(\tilde{\xi})\big] \;\geq\; \max_{f_l\in U_l} \phi_{t_g}\big(\mathbb{E}_{f_l}[\tilde{\xi}]\big) = q(m_l-t_g)^+ + b(t_g-m_l)^+ =: \Phi_{t_g}(m_l).$$

Hence

$$\sum_{l:\, x_{lg}=1} p_l\Phi_{t_g}(m_l) \;\geq\; b\sum_{l:\, x_{lg}=1} p_l(t_g-m_l)^+ \;+\; q\sum_{l:\, x_{lg}=1} p_l(m_l-t_g)^+.$$

Since all terms are nonnegative, keeping only the extreme means yields

$$\sum_{l:\, x_{lg}=1} p_l\Phi_{t_g}(m_l) \;\geq\; b \sum_{\substack{l:\, x_{lg}=1\\ m_l=m_{\min}(g)}} p_l\left(t_g-m_{\min}(g)\right)^+ \;+\; q \sum_{\substack{l:\, x_{lg}=1\\ m_l=m_{\max}(g)}} p_l\left(m_{\max}(g)-t_g\right)^+.$$

For any t_g, maximizing over $\boldsymbol{p}$ on both sides gives two valid lower bounds,

$$\max_{\boldsymbol{p}} \sum_{l:\, x_{lg}=1} p_l\Phi_{t_g}(m_l) \;\geq\; b\,\overline{p}_{\min}(g)\,(t_g-m_{\min}(g))^+,\; \max_{\boldsymbol{p}} \sum_{l:\, x_{lg}=1} p_l\Phi_{t_g}(m_l) \;\geq\; q\,\overline{p}_{\max}(g)\,(m_{\max}(g)-t_g)^+.$$

Therefore, for every t_g,

$$\max_{\boldsymbol{p}} \sum_{l:\, x_{lg}=1} p_l\Phi_{t_g}(m_l) \;\geq \max\Big\{ b\,\overline{p}_{\min}(g)\,(t_g-m_{\min}(g))^+,\; q\,\overline{p}_{\max}(g)\,(m_{\max}(g)-t_g)^+\Big\}. \tag{26}$$

Denote the right-hand side of (26) as $F(t_g)$, and minimize $F(t_g)$ over $t_g \in \mathcal{T}$. If $t_g < m_{\min}(g) < m_{\max}(g)$ then $F(t_g) = q\,\overline{p}_{\max}(g)\,(m_{\max}(g)-t_g) \geq q\,\overline{p}_{\max}(g)\,(m_{\max}-m_{\min}) = F(m_{\min}(g))$, which shows that $F(t_g)$ is decreasing on $t_g \in (0, m_{\min}(g))$. Similarly, if $t_g > m_{\max}(g) > m_{\min}(g)$ then $F(t_g) = b\,\overline{p}_{\min}(g)\,(t_g-m_{\min}(g)) \geq b\,\overline{p}_{\min}(g)\,(m_{\max}-m_{\min}) = F(m_{\max}(g))$, which shows that $F(t_g)$ is increasing on $t_g \in (m_{\max}(g), T]$. Thus, the minimizer lies in the range $[m_{\min}(g), m_{\max}(g)]$.

On this interval, $F(t_g)$ is the maximum of two affine functions:

$$F(t_g) = \max\big\{ b\,\overline{p}_{\min}(g)\,(t_g-m_{\min}),\; q\,\overline{p}_{\max}(g)\,(m_{\max}-t_g)\big\}.$$

The minimum of the maximum of these two affine functions on a closed interval is attained at the intersection point of these two lines if such a point lies within the interval. Solving

$$b\,\overline{p}_{\min}(g)\,(t_g-m_{\min}) = q\,\overline{p}_{\max}(g)\,(m_{\max}-t_g)$$

gives us

$$t_g^* = \frac{b\,\overline{p}_{\min}(g)m_{\min}(g) + q\,\overline{p}_{\max}(g)m_{\max}(g)}{b\,\overline{p}_{\min}(g) + q\,\overline{p}_{\max}(g)} \in [m_{\min}(g), m_{\max}(g)].$$

Therefore, at this point,

$$\min_{t_g \in [m_{\min}(g), m_{\max}(g)]} F(t_g) = F(t_g^*) = \frac{b\,\overline{p}_{\min}(g) q\,\overline{p}_{\max}(g)}{b\,\overline{p}_{\min}(g) + q\,\overline{p}_{\max}(g)}(m_{\max}(g) - m_{\min}(g))$$

As a result, the problem (10) is bounded below by $\min_{t_g} F(t_g) = \frac{b\,\overline{p}_{\min}(g) q\,\overline{p}_{\max}(g)}{b\,\overline{p}_{\min}(g)+q\,\overline{p}_{\max}(g)}(m_{\max}(g) - m_{\min}(g))$. □

A.8 Proof for Proposition 3

Proof. Suppose we are given $t_g \in \mathcal{T}$. For any $\tilde{\xi}$, $q(\tilde{\xi} - t_g)^+ + b(t_g - \tilde{\xi})^+ \leq \max\{b, q\}\,|\tilde{\xi} - t_g|$. Therefore, for each l,

$$\begin{aligned}
\Pi_l(t_g) &\leq \max\{b, q\} \max_{f_l \in U_l} \mathbb{E}[\big|\tilde{\xi} - t_g\big|] \\
&\leq \max\{b, q\} \left(\max_{f_l \in U_l} \mathbb{E}[|\tilde{\xi} - m_l|] + |m_l - t_g| \right) \qquad \text{(triangle inequality in } L^1) \\
&\leq \max\{b, q\} \Big(\max_{f_l \in U_l} \sqrt{\mathbb{E}[\tilde{\xi} - m_l]^2} + |m_l - t_g| \Big) \qquad \text{(Cauchy–Schwarz)} \\
&\leq \max\{b, q\} \Big(\sigma_l + |m_l - t_g| \Big).
\end{aligned}$$

Therefore, for each group g,

$$\begin{aligned}
\sum_{l:\, x_{lg}=1} p_l\,\Pi_l(t_g) &\leq \max\{b, q\} \left(\sum_{l:\, x_{lg}=1} p_l \sigma_l + \sum_{l:\, x_{lg}=1} p_l |m_l - t_g| \right) \\
&\leq \max\{b, q\}\, y_g \left(\sigma_{\max}(g) + \max_{l:\, x_{lg}=1} |m_l - t_g| \right). \qquad (27)
\end{aligned}$$

We then take the minimum over t_g. Suppose $t_g \leq m_{\min}(g)$, we have $\max_{l: x_{lg}=1} |m_l - t_g| = m_{\max}(g) - t_g \geq m_{\max}(g) - m_{\min}(g)$. Similarly, suppose $t_g \geq m_{\max}(g)$, we have $\max_{l: x_{lg}=1} |m_l - t_g| = t_g - m_{\min}(g) \geq m_{\max}(g) - m_{\min}(g)$. Therefore, the right-hand side of (27) achieves the minimum when $t_g \in [m_{\min}(g), m_{\max}(g)]$. Within this interval, $\min_{t_g \in [m_{\min}(g), m_{\max}(g)]} \max_{l: x_{lg}=1} |m_l - t_g| = \max\{t_g - m_{\min}(g), m_{\max}(g) - t_g\}$, and the minimizer is obtained when two terms are equal, i.e., $t_g = \frac{m_{\min}(g)+m_{\max}(g)}{2}$. Plugging this into the right-hand side of (27) yields

$$\min_{t_g} \max_{p \in \Delta_g} \sum_{l:\, x_{lg}=1} p_l\,\Pi_l(t_g) \;\leq\; y_g \max\{b, q\Big(\sigma_{\max}(g) + \tfrac{1}{2}\big(m_{\max}(g) - m_{\min}(g)\big)\Big).$$

This completes the proof. □

B Comparison of Different Input Features for Heuristics

We compare the results of different input features for K-Means and K-Medoids heuristics when $\rho = 0.1$ in Tables 15 and 16.

Table 15: Comparison of different input features for K-Means when $\rho = 0.1$

Feature	IS	OOS	CV Time (sec.)	Solve Time (sec.)	Total Time (sec.)
(m_l, σ_l, s_l)	4501.05	4444.69	1.20	0.05	1.25
(m_l)	4527.38	4452.32	1.20	0.06	1.26
(σ_l)	4597.18	4499.95	1.19	0.05	1.24
(s_l)	4616.57	4477.08	1.20	0.06	1.26
(m_l, σ_l)	4524.63	4459.03	1.20	0.05	1.25
(m_l, s_l)	4513.48	**4433.79**	1.22	0.05	1.27
(σ_l, s_l)	4513.57	4466.95	1.20	0.05	1.25

Table 16: Comparison of different input features for K-Medoids when $\rho = 0.1$

Feature	IS	OOS	CV Time (sec.)	Solve Time (sec.)	Total Time (sec.)
(m_l, σ_l, s_l)	4692.99	**4485.05**	0.83	0.04	0.87
(m_l)	4625.24	4493.93	0.83	0.04	0.87
(σ_l)	4655.13	4520.65	0.83	0.03	0.86
(s_l)	4712.51	4513.85	0.84	0.04	0.88
(m_l, σ_l)	4668.22	4495.23	0.85	0.04	0.89
(m_l, s_l)	4639.48	4498.57	0.83	0.04	0.87
(σ_l, s_l)	4656.40	4517.69	0.83	0.05	0.88

C Results from different ρ for one run

We investigate how the optimal solutions and optimal cost change for different ρ in a single run in Table 17.

Table 17: Results across different ρ values with a fixed seed.

ρ	Optimal duration (min.)	IS	OOS	Runtime (sec.)
0	$164(1),\ 516(2,3,4,5)$	**5112.99**	6125.17	0.96
0.1	$164(1),\ 512(2,3,4,5)$	5155.85	6101.67	1.62
0.5	$164(1),\ 466(2,3,4),\ 541(4)$	5202.27	5966.09	1.01
1.0	$164(1),\ 455(2,3,4),\ 541(4)$	5214.00	**5916.96**	0.97

Table 17 shows that although sometimes the assignments x_{lg}, y_g remain unchanged when ρ increases - for example, both $\rho = 0.5$ and $\rho = 1.0$ keep the same grouping assignments, the corresponding optimal treatment time t_g^* and IS cost still shift. This is because the grouping decision variables x_{lg}, y_g are discrete choices that govern the trade-off between the fixed assignment cost of opening another group and the variability among the modes in that group. Therefore, a small increase in ρ could not be enough to change the grouping. However, the increase in the size of the ambiguity set allows re-weighting the modes, assigning more probability mass to those with higher costs to obtain the worst-case cost so that we can minimize. As a result, different results can be achieved even if the groupings are the same. The run time comparison is inconclusive since adding more mode probabilities as ρ increases changes the problem constraints and doesn't increase monotonically.

D MMA-DRO$^{\text{mis}}$ Problem

We relax the ambiguity set U_l in (15) to allow a wider range of distributions and thus a more robust model as follows

$$
\begin{aligned}
\Pi_l(t_g) = \quad & \max_{\pi_{lk}} \sum_{k=1}^{K} \pi_{lk} \left(q(\xi_{lk} - t_g)^+ + b(t_g - \xi_{lk})^+ \right) \\
\text{s.t.} \quad & \sum_{k=1}^{K} \pi_{lk} = 1, \\
& \sum_{k=1}^{K} \pi_{lk} \xi_{lk} \leq m_l(1+\delta), \\
& \sum_{k=1}^{K} \pi_{lk} \xi_{lk} \geq m_l(1-\delta), \\
& \sum_{k=1}^{K} \pi_{lk} (\xi_{lk} - m_l)^2 \leq \sigma_l^2 (1+\delta), \\
& \sum_{k=1}^{K} \pi_{lk} (\xi_{lk} - m_l)^2 \geq \sigma_l^2 (1-\delta), \\
& \frac{1}{\sigma_l^2} \left(\sum_{k=1}^{K} \pi_{lk} (\xi_{lk} - m_l)^{+2} - \sum_{k=1}^{K} \pi_{lk} (m_l - \xi_{lk})^{+2} \right) \leq s_l(1+\delta), \\
& \frac{1}{\sigma_l^2} \left(\sum_{k=1}^{K} \pi_{lk} (\xi_{lk} - m_l)^{+2} - \sum_{k=1}^{K} \pi_{lk} (m_l - \xi_{lk})^{+2} \right) \geq s_l(1-\delta), \\
& \pi_{lk} \geq 0, \ \forall k \in \mathcal{K}.
\end{aligned} \tag{28}
$$

Because an exact continuous formulation is unavailable, we discretize the distribution on a finite support set $\Xi \in \mathbb{R}^{\mathcal{L} \times \mathcal{K}}$. Similar to Theorem 1, we derive the dual formulation and construct the MMA-DRO$^{\text{mis}}$ model.

Assign dual variables γ_{lg}, ν_{lg}^1, ν_{lg}^2, κ_{lg}^1, κ_{lg}^2, ζ_{lg}^1, ζ_{lg}^2 to the constraints in (28), we formulate the MMA-DRO$^{\text{mis}}$ problem as follows

$$
\begin{aligned}
\min \quad & \left\{ \sum_{g \in \mathcal{G}} c_g y_g + \frac{1}{\sum_{g \in \mathcal{G}} y_g} \sum_{g \in \mathcal{G}} \Big(\mu_g y_g + \sum_{l=1}^{L} \lambda_{lg} x_{lg} + \sum_{l=1}^{L} (\alpha_{lg} - \beta_{lg}) \hat{p}_l x_{lg} + \tau_g (\rho \sum_{l=1}^{L} x_{lg} \hat{p}_l) \Big) \right\} \\
\text{s.t.} \quad & \mu_g + \lambda_{lg} + (\alpha_{lg} - \beta_{lg}) (\sum_{l=1}^{L} x_{lg} \hat{p}_l) \geq \gamma_{lg} + \Big((1-\delta)\nu_{lg}^1 - (1-\delta)\nu_{lg}^2 \Big) m_l + \Big((1-\delta)\kappa_{lg}^1 - (1-\delta)\kappa_{lg}^2 \Big) \sigma_l^2
\end{aligned}
$$

$$+\Big((1-\delta)\zeta_{lg}^1-(1-\delta)\zeta_{lg}^2\Big)s_l\sigma_l^2,\ \forall l\in\mathcal{L},\ g\in\mathcal{G}$$

$$\gamma_{lg}+(\nu_{lg}^1-\nu_{lg}^2)\xi_{lk}+(\kappa_{lg}^1-\kappa_{lg}^2)(\xi_{lk}-m_l)^2+\frac{1}{\sigma^2}(\zeta_{lg}^1-\zeta_{lg}^2)\left((\xi_{lk}-m_l)^{+2}-(m_l-\xi_{lk})^{+2}\right)$$

$$\geq q(\tilde{\xi}-t_g)^+ + b(t_g-\tilde{\xi})^+,\ \forall l\in\mathcal{L},\ \forall g\in\mathcal{G},\ \forall k\in\mathcal{K}$$

$$-\alpha_{lg}-\beta_{lg}+\tau_g\geq 0,\ \forall l\in\mathcal{L},\ g\in\mathcal{G}$$

Constraints (1b), (1c), (1d), (1e)

$$\nu_{lg}^1,\ \nu_{lg}^2,\ \kappa_{lg}^1,\ \kappa_{lg}^2,\ \zeta_{lg}^1,\ \zeta_{lg}^2,\ \lambda_{lg},\ \alpha_{lg},\ \beta_{lg},\ \tau_g,\ t_g\geq 0$$

$$\gamma_l,\ \mu_g\in\mathbb{R}$$

$$x_{lg},\ y_g\in\{0,1\},\ \forall l\in\mathcal{L},\ g\in\mathcal{G}$$